Space microgravity improves proliferation of human iPSC-derived cardiomyocytes

Antonio Rampoldi¹, Parvin Forghani¹, Dong Li¹, Hyun Hwang¹, Lawrence Christian Armand¹,

Jordan Fite², Gene Boland², Joshua Maxwell¹, Kevin Maher¹, and Chunhui Xu^{1,3}

¹Department of Pediatrics, Emory University School of Medicine and Children's Healthcare of

Atlanta, Atlanta, GA, USA

²Techshot, Inc., Greenville, IN, USA

³Wallace H. Coulter Department of Biomedical Engineering, Georgia Institute of Technology and

Emory University, Atlanta, GA, USA

Running title: Cardiac differentiation in space microgravity

Correspondence: chunhui.xu@emory.edu

1

SUMMARY

In microgravity, cells undergo profound changes in their properties. However, how human cardiac progenitors respond to space microgravity is unknown. In this study, we evaluated the effect of space microgravity on differentiation of hiPSC-derived cardiac progenitors compared with 1G cultures on the International Space Station (ISS). Cryopreserved 3D cardiac progenitors were cultured for 3 weeks on the ISS. Compared with 1G cultures, the microgravity cultures had 3-fold larger sphere sizes, 20-fold higher counts of nuclei, and increased expression of proliferation markers. Highly enriched cardiomyocytes generated in space microgravity showed improved Ca²⁺ handling and increased expression of contraction-associated genes. Short-term exposure (3 days) of cardiac progenitors to space microgravity upregulated genes involved in cell proliferation, survival, cardiac differentiation and contraction, consistent with improved microgravity cultures at the late stage. These results indicate that space microgravity increased proliferation of hiPSC-cardiomyocytes, which had appropriate structure and function.

Key Words: cardiomyocytes, differentiation, function, human induced pluripotent stem cells, microgravity, proliferation

INTRODUCTION

A leading candidate cell source for regenerative cardiac therapy is the cardiomyocytes derived from human induced pluripotent stem cells (hiPSC-CMs) (Laflamme and Murry, 2005). Targeting the intermediate steps from hiPSCs to cardiomyocytes could help improve the efficiency of hiPSC-CM production. Exposure of cardiac progenitors to microgravity presents a novel method to achieve cardiomyocyte differentiation at high efficiency and high yield, as microgravity can profoundly modulate cell properties (Barzegari and Saei, 2012; Becker and Souza, 2013; Ingber, 1999) including proliferation of stem cells (Chen et al., 2006; Kawahara et al., 2009; Li et al., 2009). For example, under simulated microgravity generated with a random positioning machine, microscale 3-dimensional (3D) cardiac progenitors from hiPSCs showed increased proliferation and survival compared with parallel cultures under standard gravity (Jha et al., 2016), resulting in the production of enriched cardiomyocytes at high cell yield. These cardiomyocytes also had improved structural and functional maturation features (Jha et al., 2016), which are highly desirable for improving the safety of cell therapy since transplantation of immature cardiomyocytes increases the risk of graft-induced arrhythmias (Chong et al., 2014).

The International Space Station (ISS)-U.S. National Laboratory provides an extraordinary environment to study the effect of space microgravity on cell properties that is not achievable elsewhere. While the random positioning machine and similar devices can simulate some aspects of microgravity and weightless environment during spaceflight, they only provide a good approximation to microgravity environment on Earth (Grimm et al., 2014; Zhang et al., 2013). Gravitational forces are still present under simulated microgravity, affecting cell properties. Research on the ISS has shown that space microgravity can indeed modulate cell properties (Unsworth and Lelkes, 1998) and provide beneficial effects on the cells for possible therapeutic use on Earth (Freed and Vunjak-Novakovic, 2002; Sharma et al., 2022; Yuge et al., 2006).

Cell biology studies on the ISS are usually conducted using live, non-cryopreserved cell cultures maintained in modules that required CO₂ (Wnorowski et al., 2019). To facilitate the study of space microgravity on the culture and differentiation of 3D cardiac progenitors, we have recently developed methods to cryopreserve the 3D cardiac progenitors and culture them in a CO₂-

independent medium (Rampoldi et al., 2021). In this study, we conducted a spaceflight experiment (MVP-CELL-03 project) with cryopreserved hiPSC-derived cardiac progenitors sent to the ISS through the SpaceX-20 mission. The astronauts successfully cultured the cells for 3 weeks and returned live beating cardiomyocytes back to us. We then comprehensively assessed the cellular, molecular, and functional characteristics of the cells. We also assessed the molecular effect of a short-term (3 days) exposure of cardiac progenitors to space microgravity. Here, we report that space microgravity increased cell proliferation and that the cardiomyocytes generated in space microgravity cultures showed appropriate structural and functional features.

RESULTS

Recovery of live cells following cell culture of cryopreserved 3D cardiac progenitors without CO₂ on the ISS

For the spaceflight experiment (MVP-CELL-03 project), we prepared cryopreserved cardiac progenitor spheres from two hiPSC lines: SCVI-273 and IMR90 (Figure S1 and Supplemental Results). The cryopreserved cardiac progenitors were flown to the ISS through the SpaceX-20 mission. As illustrated in Figure 1A, the astronauts on board the ISS thawed the cardiac progenitor spheres into the CO₂-independent medium with a ROCK inhibitor. The cells were cultured at 37°C using the Multi-specimen Variable-gravity Platform (MVP) configured to load multiple cultures under both ISS microgravity (ISS μG) and ISS 1G conditions; the 1G condition on the ISS was achieved by centrifugation of one carousel within the same MVP system (Figure 1B-C). Specifically, we designed our experiments to examine the growth and differentiation of 3D cardiac progenitors from two hiPSC cell lines under ISS μG and ISS 1G conditions with each condition run in triplicates. A total of 12 MVP experiment modules (6 for each cell line) were used.

For short-term exposure of microgravity, after 3 days of cell culture on the ISS, an aliquot of samples was harvested from the experimental modules, fixed using RNAProtect, and stored at - 20°C. For long-term exposure of space microgravity, live cultures were returned to ground via warm storage after having been cultured for 22 days on the ISS for further analysis. The cardiac

spheres from post-flight ISS cultures recovered beating activity 2-3 days after they were transferred to an incubator, with beat rates of 10-15 beats/min in ISS 1G cultures and 9-17 beats/min in ISS µG cultures.

Space microgravity increases the size of hiPSC-CM spheres and hiPSC-CM proliferation Cardiac sphere morphology was examined under a phase-contrast microscope after the samples were returned from the ISS. Phase-contrast photos were taken (Figure 2A) and sphere diameters were measured by software ImageJ. In the IMR90 ISS µG cultures, cardiac spheres were on average 3 times bigger in size compared with ISS 1G cardiac spheres (Figure 2B). Similar results were observed in the SCVI-273 ISS cultures (Figure 2A, 2B).

Immunocytochemical analysis was performed to examine cardiomyocyte purity and cardiomyocyte proliferation of the ISS cultures. As shown in Figure 2C-D, the majority of the cells were positive for NKX2.5 (>95%) in both ISS 1G and μG conditions. These results were similar to the pre-testing results done before the samples were flown to the ISS (Figure S1C-D). In addition, approximately 7% of cells were positive for Ki-67 in ISS μG cultures, while no Ki-67-positive cells were detected in ISS 1G cultures (Figure 2C-D). As expected, almost all cells were positive for cardiac marker cTNI in both ISS μG and ISS 1G cultures. Therefore, ISS cultures of the cryopreserved cardiac progenitor spheres differentiated into highly enriched cardiomyocytes, and ISS μG cultures contained more cells at the active phase of cell cycle than did ISS 1G culture.

We examined the expression of genes related to cell cycle and cell proliferation in both short-term (3 days) and long-term (3 weeks) ISS cultures by qRT-PCR analysis (Figure 2E). The expression of CCND2 (cyclin D2), CCND1 (cyclin D1), TBX3 (T-box transcription factor 3) and IGF2 (insulin like growth factor 2) was significantly upregulated in ISS μ G cells compared with ISS 1G cells from both short-term and long-term cultures. Compared with the short-term ISS μ G cultures, the long-term ISS μ G cultures had increased expression of CCND1 and IGF2. In addition, the nuclei counts of live cells (after the long-term culture cells were replated) were ~20 times higher in cells from ISS μ G cultures compared with ISS 1G cultures (Figure 2F). These results were consistent with the observations on increased proliferation capacity in ISS μ G cells.

Space microgravity improves cellular and structural parameters in hiPSC-CMs

Immunocytochemical analysis was performed in ISS μ G and ISS 1G cultures for other cardiac structural markers including α -actinin, cTNT (cardiac troponin T) and pan-cadherin (Figure 3A). Almost all cells from ISS μ G and ISS 1G cultures were positive for these cardiac structural markers. ISS μ G cells had larger cell area but similar perimeter compared with ISS 1G control. In addition, ISS 1G cells were more elongated, while ISS μ G cells expanded in both length and width (Figure 3B).

We evaluated cells for their overall appearance of sarcomeric striations based on the levels of the organization of the Z-line protein α -actinin and categorized them into 3 different levels as described previously (Jha *et al.*, 2016; Nguyen et al., 2014; Ribeiro et al., 2015). As shown in Figure 4A, cells with Score 1 were α -actinin positive cells but without clear sarcomeric striations; cells with Score 2 were cells with a diffuse and punctate staining pattern of α -actinin staining; and cell with Score 3 were cells with more organized myofibrillar structure with distinct paralleled bands of z-discs. Compared with ISS 1G cardiomyocytes, cardiac spheres exposed to space microgravity had more cells with a higher score of defined myofibrillar structure, indicating an improved structural development (Figure 4A).

In addition, we examined the expression of genes related to cardiac structural proteins in intact cardiac spheres. Among the genes examined, *MYL2* (myosin light chain 2V, an isoform in more mature cardiomyocytes), *TNNI3* (cardiac troponin I3, an isoform in more mature cardiomyocytes), *MYH6* (myosin heavy chain 6), and *MYH7* (myosin heavy chain 7, an isoform in more mature cardiomyocytes) were upregulated in ISS μG cells compared with ISS 1G cells from both short-term (3 days) and long-term (3 weeks) ISS cultures (Figure 4B). In long-term ISS cultures, *MYL7* (myosin light chain 2A) and *TNNT2* (cardiac troponin T2) were also upregulated in ISS μG cells compared with ISS 1G cells. In addition, compared with the short-term ISS μG cells, the long-term ISS μG cells had increased expression of *TNNT2* and *TNNI3*. Such increased cardiac structural proteins are major parameters of cardiomyocyte maturation (Guo and Pu, 2020).

Space microgravity improves Ca2+ signaling in hiPSC-CMs

After the cardiac spheres were transferred to low adhesion dishes, ISS μ G cardiac spheres recovered beating activity quite fast, between 16 h to 36 h. In ISS 1G cultures, spheres showed beating activity 48 h after being transferred. To assess the function of hiPSC-CMs from the ISS cultures at single cell level, we performed Ca²⁺ signaling analysis after the cardiac spheres were dissociated and replated. The cells recovered beating activity after they were maintained in RPMI 1640 with 2% B27 supplement for 72 h, and were then loaded with calcium-sensitive dye Fluo-4 for Ca²⁺ imaging.

Among these beating cells, we observed 3 types of Ca²⁺ transients: (1) normal Ca²⁺ transients, (2) abnormal Ca²⁺ transients with spontaneous Ca²⁺ leak showing a single notch of diastolic Ca²⁺ signal, and (3) abnormal Ca²⁺ transients with inconsistent beating period (Figure 5A). Transients were categorized as "normal" if they had mostly consistent amplitudes and beat periods with typical cardiac transient morphology of upstroke and decay kinetics, while transients were categorized as "abnormal" if they exhibited spontaneous Ca2+ release between transients oscillations of diastolic cytosolic Ca²⁺ and inconsistent beating (Preininger et al., 2016). ISS µG samples had more cells with normal Ca2+ transients compared with ISS 1G samples (93% in ISS μG cells vs. 78% in ISS 1G cells) (Figure 5B). The proportion of the cells with abnormal Ca²⁺ transients and the types of abnormal Ca²⁺ transients in ISS 1G cultures were comparable to typical hiPSC-CM cultures in ground-based studies (Forghani et al., 2021; Lan et al., 2013; Liu et al., 2020a; Saraf et al., 2021). Most of these abnormal cells had minor abnormality with inconsistent beating period (Type B) and a few cells had transients with a single notch of additional Ca2+ spike (diastolic Ca²⁺ signal) before the following Ca²⁺ transient had initiated (Type A) (Figure 5A, 5B). These minor abnormal types of Ca²⁺ transients are likely due to immature nature of hiPSC-CMs. In both ISS µG and ISS 1G samples, we did not observe cells with other types of abnormal Ca²⁺ transients associated with arrhythmias such as tachycardia-like events or transients with multiple notches of additional Ca²⁺ spikes as in hiPSC-CMs from patients with heart disease or hiPSC-CMs treated with drugs.

Among the cells with normal Ca²⁺ transients, ISS µG cells had reduced time to peak, increased peak amplitude, reduced half width, and increased maximum rise slope and maximum decay slope compared with ISS 1G cells (Figure 5C), indicating faster Ca²⁺ transient kinetics, a functional feature of more mature cardiomyocytes.

In addition, the expression of calcium handling proteins/ion channels (*CASQ2* [calsequestrin 2] and *ATP2B4* [ATPase plasma membrane Ca²⁺ transporting 4]) was significantly upregulated in ISS μG cardiac spheres compared with ISS 1G cardiac spheres from both short-term (3 days) and long-term (3 week) ISS cultures (Figure 5D).

These results suggest that space microgravity reduced abnormal Ca²⁺ signaling and increased Ca²⁺ handling kinetics, which was consistent with increased expression of Ca²⁺ handling proteins in ISS 1G cells.

RNA-seq analysis reveals increased proliferation and differentiation during short-term exposure to space microgravity

We next examined how a short-term exposure of cardiac progenitors to space microgravity affected the expression of genes associated with expansion and differentiation of these cells. Using cardiac spheres collected 3 days after thawing onboard the ISS, we performed RNA-seq analysis to compare global gene expression profiles of SCVI-273 hiPSC-CMs in ISS µG vs. ISS 1G conditions. As detected by RNA-seq, 195 genes were significantly upregulated and 207 downregulated in ISS µG cells compared with ISS 1G cells. Among the significantly upregulated genes (Figure 6A & Table S1), several are involved in cell cycle, proliferation, survival, and regeneration. They include *CCNB3* (cyclin B3) which promotes metaphase-anaphase transition in cell cycle (Li et al., 2019); *RELN* (reelin) which promotes cardiac regeneration and repair by improving cell survival after heart injury (Liu et al., 2020b), and *UBR3* (ubiquitin protein ligase E3 component N-recognin 3) which regulates APE1 (apurinic/apyrimidinic endodeoxyribonuclease 1), a protein involved in DNA damage repair, cell survival, and regulation of transcription, to reduce genome instability (Meisenberg et al., 2012).

Several upregulated genes are also involved in heart development. They include *LMO7* (Lim-domain only 7), a transcriptional regulator of emerin involved in beta-catenin signaling (Holaska et al., 2006); *COL14A1* (collagen type XIV alpha 1), encoding type XIV collagen which is important for growth and structural integrity of the myocardium (Tao et al., 2012); *HSPG2* (heparan sulfate proteoglycan 2), encoding protein perlecan (a major structural components of the basement membrane surrounding cells in the myocardium (Martinez et al., 2018)). Several other genes are also involved in modulating cardiomyocyte contractility. They include *CXCR4* (C-X-C motif chemokine receptor 4) (Pyo et al., 2006) and *GJA5* (gap junction protein alpha 5) (Chaldoupi et al., 2009) which are responsible for contraction and the electrical coupling of cardiomyocytes. Space microgravity also increased the expression of genes involved in fatty acid metabolism, including *TECRL* (trans-2,3-enoyl-CoA reductase like), whose mutations are linked to catecholaminergic polymorphic ventricular tachycardia (Moscu-Gregor et al., 2020).

Among significantly downregulated genes (Figure 6A & Table S1), *MT-RNR1* (mitochondrially encoded 12S RRNA) and *MT-RNR2* (mitochondrially encoded 16S RRNA) are functional ncRNAs that protect cells from mitochondrial apoptosis (Bitar et al., 2017); *MT-RNR1* was upregulated in hiPSC-CMs subjected to ionizing radiation during differentiation (Baljinnyam et al., 2017). Another downregulated gene, *ANGPT2* (cytokine angiopoietin-2), is a promising predictor of heart disease (Pöss et al., 2015) and possesses proinflammatory and apoptosis-promoting abilities (Scholz et al., 2015). Other downregulated genes are involved in the Jak-Stat-and MAPK-pathways. They include *DUSP*1 (dual specificity phosphatase 1) and *DUSP2* (dual specificity phosphatase 2), encoding a subclass of tyrosine phosphatases that regulate the activity of MAPK, mediating stress responses, inflammation and apoptosis (Lang and Raffi, 2019); and *SERPINE1* (serpin family E member 1), a serine protease inhibitor of plasminogen activator and an activator of the JAK/STAT pathway associated with cellular stress (Simone et al., 2014) and cardiac diseases (Basisty et al., 2020).

According to Gene Set Enrichment Analysis (GSEA), space microgravity upregulated the GO terms of biological processes associated with cardiac muscle cell development, muscle activity or cell contractions (Figure 6B; Supplemental Results) and the GO terms of cellular components

and molecular functions associated with structural constituent of muscle, sarcomeric structure and voltage-gated calcium channel activity involved in cardiac muscle cell action potential and sodium channel activity (Figure S2; Supplemental Results). In addition, space microgravity downregulated GO terms associated with processes, functions or components of non-cardiac cells, like nephron development and neuronal cell body (Figures 6B and S2; Supplemental Results). These results were consistent with efficient differentiation and maturation of ISS µG cells into cardiomyocytes.

We next examined the link between selected GO terms of biological processes and specific differentially expressed genes (Figure 7; Supplemental Results). Notably, ISS μ G cells had upregulated GO term of cyclin-dependent protein serine/threonine kinase regulator activity that was linked to upregulated genes of *CCNB3* and *CCND2*. Among upregulated genes, *CCNB3* had the highest increase in ISS μ G cultures (log₂[fold change] = 7.25) (Table S1). *CCNB3* is known to regulate the G2/M transition of mitotic cells (Li *et al.*, 2019), whereas *CCND2* regulates the G1/S and its overexpression is associated with increased survival and regeneration potency in hiPSC-CMs (Zhu *et al.*, 2018). In addition, cellular amino acid biosynthetic process and the tricarboxylic acid cycle were also upregulated, indicating that ISS μ G cells were metabolically more activate than ISS 1G cells.

KEGG enrichment analysis showed that several pathways were upregulated by space microgravity, including calcium signaling pathway, cardiac muscle contraction, and adrenergic signaling in cardiomyocytes, which is tightly connected to calcium signaling, cell contraction and cardiomyocyte maturation. Regulations of the specific genes associated with these pathways and cell cycle are shown in Figures S3-5. The MAPK signaling pathway and ribosomal subunits proteins were downregulated in ISS μ G cells (Figures S6-7). Since cell differentiation is associated with the downregulation of rRNA transcription (Hayashi et al., 2014), these results suggest that ISS μ G cells actively differentiated into cardiomyocytes.

Together, both the GO term and KEGG enrichment analyses indicate that ISS μ G cells were in a state of increased cell growth and cardiac differentiation compared with ISS 1G cells.

DISCUSSION

Despite recent advances in understanding cell behavior under extracellular forces, few studies have investigated changes in proliferation and differentiation of cells under space microgravity (Baio et al., 2018b; Huang et al., 2020; Wnorowski *et al.*, 2019). Our analysis shows that the expansion of hiPSC-derived cardiac progenitors under space microgravity resulted in increased cell proliferation and efficient generation of highly enriched cardiomyocytes with appropriate features. Specifically, the beating cardiac spheres were detected in the cultures, containing >90% cardiomyocytes. Compared with cells from ISS 1G cultures, cardiac spheres from ISS μG cultures were bigger in size and had appropriate molecular and functional properties. At single cell level, cells from ISS μG cultures had increased cell size and clearer sarcomere structure. The cells also had an increased peak amplitude and faster kinetics of Ca²⁺ transients. RNA-seq analysis showed upregulation of genes associated with cardiac development, cell cycle, proliferation, survival, and cardiac functions, and downregulation of genes related to extracellular matrix and apoptosis in ISS μG cultures compared with ISS 1G cultures.

An innovative aspect of this study is the direct comparison of cells cultured under both µG condition and 1G condition in the MVP system on the ISS. Unlike typical ISS experiments where microgravity cells are compared with the ground control, the MVP system consisted of both ISS µG and ISS 1G modules and thus allowed us to better characterize the impact of space microgravity alone on physiology, structure and gene expression of hiPSC-CMs and examine whether space microgravity altered the growth and differentiation of cardiac progenitors. Therefore, we could focus on the effect of space microgravity without background noise of space environment, including space radiation that could potentially alter or mask microgravity effects on cellular features and gene expression. The MVP system had automatic imaging device for each cell culture module but did not provide clear images for us to monitor the presence of beating cells. Further improvement of the flight hardware with more advanced and automatic imaging with higher resolutions would be desirable.

Multiple assessments indicate that long-term exposure of cardiac progenitors to space microgravity generated enriched cardiomyocytes with improved proliferation. The size of the spheres under ISS µG was 3 times bigger on average than that of ISS 1G controls. Compared with

ISS 1G cultures, ISS μ G cultures also had increased features of proliferation, including increased expression of proliferation marker Ki-67: 7% of ISS μ G cells were positive for Ki-67, while Ki-67 was not detected in ISS 1G cultures. These results were further confirmed by upregulation of selected genes in ISS μ G cultures, including *TBX3* (Ribeiro et al., 2007), *IGF2* (Shen et al., 2020), *CCND1* (Gan et al., 2019) and *CCND2* (Zhu et al., 2018), which have specific roles in cell cycle, cell proliferation and heart regeneration. Furthermore, the counts of live cell nuclei in ISS μ G cultures were 20-fold higher than those in ISS 1G cultures.

Both structural and functional assessments indicate that cardiomyocytes from ISS μG cultures had improved features. Cells from ISS μG cultures had increased cell size and contained more cells with better-developed and clearer sarcomere compared with cells from ISS 1G cultures and therefore were structurally improved. The improved cardiomyocyte structure could contribute to the increased stability of Ca²⁺ signaling we observed in ISS μG cells—the proportions of the cells with normal Ca²⁺ transients were higher in ISS μG cells than in ISS 1G cells. ISS μG cells also had an increased peak amplitude and faster kinetics of Ca²⁺ transients. Consistently, ISS μG cells had increased expression of genes encoding cardiac structural and Ca²⁺ handling proteins including *MYL2*, *MYL7*, *TNNI3*, *TNNT2*, *MYH6*, *MYH7*, *CASQ2* and *ATP2B4*, indicating that space microgravity could have a beneficial effect on the structure and function of cardiac cells.

Following the sampling of SCVI-273 cultures at day 3 for RNA-seq analysis, only a limited amount of the cells was left for late-stage characterization. Because of this limitation, our characterization of the late-stage cells was focused on the IMR90 cultures but not the SCVI-273 cultures. However, the cell morphologies of both the cell lines were similar at the late stage. In addition, molecular profiling of the short-term cultures of SCVI-273 cells reveals gene regulations that are consistent with the improved cell proliferation observed in the long-term cultures of IMR90 cells. Our RNA-seq analysis of the cardiac spheres that had short-term exposure of microgravity revealed upregulation of key genes and pathways involved in cardiomyocytes differentiation, cardiac structural maturation, contractility, and cell proliferation in ISS µG cells compared with ISS 1G cells. We also detected downregulation of genes and pathways associated with apoptosis, inflammation and cellular stress in ISS µG cells compared with ISS 1G cells. These results indicate

that the short-term exposure of cardiac progenitors to space microgravity was able to implement significant changes in their transcriptomic profiles.

Previous studies indicate that cells can undergo profound changes at the morphological, molecular and functional levels in response to microgravity and spaceflight (Freed and Vunjak-Novakovic, 2002; Unsworth and Lelkes, 1998). For example, neonatal cardiovascular progenitors (CPCs) had enhanced cell proliferation and changes in cytoskeletal organization and migration after the cells were cultured aboard the ISS for 30 days (Baio *et al.*, 2018b). These CPCs also exhibited elevated expression of Ca²⁺ handling and signaling genes, which corresponded to the activation of protein kinase C alpha, a calcium-dependent protein kinase (Baio et al., 2018a). In another spaceflight study, human mesenchymal stem cells cultured on the ISS for 7 and 14 days had more potent immunosuppressive capacity than did the ground control (Huang *et al.*, 2020). In addition, simulated microgravity potentiated the proliferation of bone marrow-derived human mesenchymal stem cells (Yuge *et al.*, 2006) and adipose-derived stem cells (Zhang et al., 2015).

Our RNA-seq results provide insights into genes and molecular pathways linked to cardiomyocyte survival and differentiation. For example, ISS μG cells had upregulated expression of genes that support cell proliferation, survival, and cardiac development, including *CCNB3*, *CCND2*, *TBX1* (T-box transcription factor 1) and *TBX2* (T-box transcription factor 2). Among them, *CCNB3* was the most upregulated gene in ISS μG cells. The role of *CCNB3* in cardiomyocyte proliferation, survival and differentiation has not been reported, although another cyclin gene *CCND2* is known to be able to improve cardiomyocyte proliferation and cardiac regeneration (Zhu *et al.*, 2018). Further study on *CCNB3* and other genes identified in our transcriptomic analysis is likely to be fruitful given significant challenge in graft survival of hiPSC-CMs for regenerative medicine—in nonhuman primate model studies, even with the prosurvival pretreatment, ~90% of the transplanted cells died post-injection (Chong and Murry, 2014).

Our RNA-seq results also highlight that the enhanced cardiomyocyte differentiation in ISS μ G cultures was associated with decreased expression of genes associated with differentiation of non-cardiac lineages. For example, the expression of genes related to the GO term of positive regulation of vasculature development and the GO terms associated with processes, functions or

components of neurons and nephrons were downregulated in ISS µG cells. Suppression of differentiation of other cell types would be expected during efficient cardiomyocyte differentiation as, for example, endothelial and cardiac cells are derived from the same progenitors. The results of the molecular profiling could be exploited to facilitate efficient production of cardiomyocytes under standard gravity. Modulating gene expression during early stage cardiomyocyte differentiation could significantly affect the efficiency of differentiation. For example, downregulation of a Wnt-signaling gene (*LGR5*, leucine rich repeat containing G protein-coupled receptor 5) inhibited cardiomyocyte differentiation but potentiated endothelial differentiation, while a typical differentiation cultures without suppression of *LGR5* resulted in higher levels of cardiomyocytes but very few endothelial cells (Jha et al., 2017).

Therapeutic application of hiPSC-CMs requires not only large amounts of the cells with improved ability for engraftment, but also cells with high quality including improved maturation and function in order to improve the safety of cell therapy. Our transcriptomic analysis showed an upregulation of genes and pathways that support cell contractility and calcium signaling. In addition to increased expression of genes associated with Ca²⁺ handling, structure and contractility in late-stage ISS μG cells, ISS μG cells at early stage had reduced expression of several genes related to potassium channel activity, including *KCNK5* (potassium two pore domain channel subfamily K member 5) and *KCNMA1* (potassium calcium-activated channel subfamily M alpha 1). Cardiac potassium channels regulate the shape and duration of the cardiac action potential, and limit the depolarization duration of the cell membrane and the time course of the contractions and the refractory periods (Tamargo *et al.*, 2004). The upregulation of genes involved in calcium channel activity related to contraction and downregulation of genes related to potassium channel activity may be in part contributing to the reduced abnormal intracellular Ca²⁺ transients observed in ISS μG cells.

In conclusion, we have demonstrated that culture of cryopreserved 3D cardiac progenitors under space microgravity resulted in efficient differentiation of cardiomyocytes. The combination of microgravity and 3D culture employed in this study provides a novel method to increase the proliferation and differentiation of cardiac progenitors. This method also results in cardiomyocytes

with improved proliferation, structure, and cardiac function, which are highly desirable for future application of hiPSC-CMs in regenerative medicine. In addition, we have identified potential genes and pathways involved in cardiomyocyte proliferation, survival and differentiation. Targeting these genes and pathways may provide alternative strategies used on Earth to mimic the effect of space microgravity on improved proliferation, survival, and differentiation of hiPSC-CMs.

EXPERIMENTAL PROCEDURES

Cell culture and cardiomyocyte differentiation

SCVI-273 and IMR90 hiPSCs were cultured in a feeder-free condition and subjected to cardiomyocyte differentiation by small molecule (Lian *et al.*, 2012) and growth factors, respectively (Jha *et al.*, 2015; Laflamme *et al.*, 2007).

Formation and cryopreservation of cardiac progenitor spheres

Cardiac progenitor spheres were generated from differentiation day 6 cultures that were dissociated using 0.25% trypsin-EDTA (Thermo Fisher Scientific). The dissociated cells were seeded into the Aggrewell 400 plates at 1.8x10⁶ cells/well (1,500 cells/microwell) and cultured in RPMI/B27 medium (RPMI 1640 with 2% B27 supplement with insulin) with 10 µM ROCK inhibitor Y-27632. After 24 h, cardiac progenitor spheres were collected and resuspended in cryopreservation medium (90% fetal bovine serum and 10% dimethyl sulfoxide with 10 µM ROCK inhibitor) and transferred into cryosyringes at 0.5 mL/cryosyringe. The cryosyringes were cooled at 4°C for 25 min and then stored at -80°C in a cooling box (Rampoldi *et al.*, 2021).

ISS cell culture facility and spaceflight operation

The cryopreserved cardiac progenitor spheres were pre-tested and sent to the ISS through the SPACEX-20 mission, a mission launched by the aerospace company SpaceX on March 6, 2020 (https://www.issnationallab.org/launches/spacex-crs-20/). On the ISS, the astronauts thawed the cryopreserved cardiac progenitor spheres, and cultured the cells using the MVP system from

Techshot, Inc. The MVP system allows loading of multiple cultures/modules under both ISS μ G and ISS 1G conditions (the 1G condition on the ISS was achieved by centrifugation). Each condition was run in triplicates for each cell line.

For thawing cells, cryosyringes containing cardiac progenitor spheres were placed in a thermoblock at 37°C for 5 min. The cells were then injected into cell culture chambers of the MVP modules containing the CO₂-independent medium with 10 µM ROCK inhibitor (Table S2) (Rampoldi *et al.*, 2021). The MVP modules were re-installed into the MVP facility, which started with a medium flush cycle to replace the medium with new culture medium (20 mL per chamber; ~2x chamber volume), to flush out the DMSO in the cryopreserved cell solution (0.5 mL/cryosyringe). The cells were cultured at 37°C in the MVP system with medium exchange every other day.

For short-term exposure of space microgravity, after 3 days of cell culture on the ISS, the following samples were harvested, fixed using RNAProtect and stored at -20°C: 3 samples from SCVI-273 hiPSCs at ISS μ G and 3 samples from SCVI-273 hiPSCs at ISS 1G (1 sample each from the 3 cell culture modules; and 9 mL for each sample). The remaining cells were returned to the MVP for the duration of the experiment. For long-term exposure of space microgravity, live cultures were returned to ground via warm storage after 22 days of culture on the ISS.

Upon arrival at Emory University, cardiac spheres were transferred immediately into an incubator and allowed to recover overnight. The following day cardiac spheres were transferred from the collection bags into low adhesion dishes in RPMI 1640 medium with 2% B27 supplement, and were then maintained overnight. Spheres were imaged using an inverted microscope (Axio Vert.A1) and analyzed by ImageJ software.

Quantification and statistical analysis

Data were analyzed in GraphPad Prism 7.04. Comparisons were conducted via an unpaired, two-tailed Student's t test and one-way ANOVA test with significant differences defined by *, P < 0.05; ***, P < 0.01; ***, P < 0.001 and ****, P < 0.0001. Data are presented as mean ± standard deviation.

Supplemental experimental procedures include cell culture, immunocytochemical analysis, high-content imaging analysis, structural analysis of hiPSC-CMs, RNA-seq analyses, quantitative real-time RT-PCR, and calcium imaging.

DATA AND CODE AVAILABILITY

The RNA-seq data have been deposited at the GEO database under accession code GSE188793.

SUPPLEMENTAL INFORMATION

Supplemental information includes Figures S1-S7, Table S1-S5, supplemental results and supplemental experimental procedures.

ACKNOWLEDGEMENTS

We thank Astronaut Jessica Meir and Astronaut Andrew Morgan for performing cell culture experiments aboard the International Space Station and Gregory Tharp and Kathryn Pellegrini at Emory University for RNA-seq analysis. We also thank Dr. Bill McLamb and Dr. Marc Giulianotti of the CASIS for guidance and discussions. The graphical abstract was created with BioRender.com. This study was supported in part by the Center for Advancement of Science in Space (GA-2017-266), the National Institutes of Health (R01HL136345 and R01AA028527), and the National Science Foundation and the Center for Advancement of Science in Space (CBET 1926387).

AUTHOR CONTRIBUTIONS

A.R., K.M. and C.X. designed experiments. A.R., P.F., D.L., H.H., L.C.A., and J.M. performed experiments and analyzed data. J.F. and G.B. contributed to the MVP hardware design and testing. A.R. and C.X. wrote the manuscript. All authors reviewed and approved the manuscript.

DECLARATION OF INTERESTS

J.F. and G.B. were employees of Techshot Inc. All other authors declare no competing interests.

REFERENCES

- Baio, J., Martinez, A.F., Bailey, L., Hasaniya, N., Pecaut, M.J., and Kearns-Jonker, M. (2018a). Spaceflight Activates Protein Kinase C Alpha Signaling and Modifies the Developmental Stage of Human Neonatal Cardiovascular Progenitor Cells. Stem Cells Dev 27, 805-818. 10.1089/scd.2017.0263.
- Baio, J., Martinez, A.F., Silva, I., Hoehn, C.V., Countryman, S., Bailey, L., Hasaniya, N., Pecaut, M.J., and Kearns-Jonker, M. (2018b). Cardiovascular progenitor cells cultured aboard the International Space Station exhibit altered developmental and functional properties. NPJ Microgravity 4, 13. 10.1038/s41526-018-0048-x.
- Baljinnyam, E., Venkatesh, S., Gordan, R., Mareedu, S., Zhang, J., Xie, L., Azzam, E., Suzuki, C., and Fraidenraich, D. (2017). Effect of densely ionizing radiation on cardiomyocyte differentiation from human-induced pluripotent stem cells. Physiol Rep *5*. 10.14814/phy2.13308.
- Barzegari, A., and Saei, A.A. (2012). An update to space biomedical research: tissue engineering in microgravity bioreactors. Bioimpacts *2*, 23-32. 10.5681/bi.2012.003.
- Basisty, N., Kale, A., Jeon, O., Kuehnemann, C., Payne, T., Rao, C., Holtz, A., Shah, S., Sharma, V., Ferrucci, L., et al. (2020). A proteomic atlas of senescence-associated secretomes for aging biomarker development. PLoS biology *18*. 10.1371/journal.pbio.3000599.
- Becker, J.L., and Souza, G.R. (2013). Using space-based investigations to inform cancer research on Earth. Nat Rev Cancer 13, 315-327. 10.1038/nrc3507.
- Bitar, M., Kuiper, S., O'Brien, E., and Barry, G. (2017). Using Human iPSC-Derived Neurons to Uncover Activity-Dependent Non-Coding RNAs. Genes 8. 10.3390/genes8120401.
- Chaldoupi, S., Loh, P., Hauer, R., De Bakker, J., and Van Rijen, H. (2009). The role of connexin40 in atrial fibrillation. Cardiovascular research *84*. 10.1093/cvr/cvp203.
- Chen, X., Xu, H., Wan, C., McCaigue, M., and Li, G. (2006). Bioreactor expansion of human adult bone marrow-derived mesenchymal stem cells. Stem Cells *24*, 2052-2059. 10.1634/stemcells.2005-0591.
- Chong, J.J., and Murry, C.E. (2014). Cardiac regeneration using pluripotent stem cells-Progression to large animal models. Stem Cell Res *13*, 654-665. 10.1016/j.scr.2014.06.005.
- Chong, J.J., Yang, X., Don, C.W., Minami, E., Liu, Y.W., Weyers, J.J., Mahoney, W.M., Van Biber, B., Palpant, N.J., Gantz, J.A., et al. (2014). Human embryonic-stem-cell-derived cardiomyocytes regenerate non-human primate hearts. Nature. 10.1038/nature13233.
- Forghani, P., Rashid, A., Sun, F., Liu, R., Li, D., Lee, M.R., Hwang, H., Maxwell, J.T., Mandawat, A., Wu, R., et al. (2021). Carfilzomib Treatment Causes Molecular and Functional Alterations of Human Induced Pluripotent Stem Cell-Derived Cardiomyocytes. J Am Heart Assoc *10*, e022247. 10.1161/JAHA.121.022247.
- Freed, L., and Vunjak-Novakovic, G. (2002). Spaceflight bioreactor studies of cells and tissues. Advances in space biology and medicine 8. 10.1016/s1569-2574(02)08019-x.
- Gan, J., Tang, F., Su, X., Lu, G., Xu, J., Lee, H., and Lee, K. (2019). microRNA-1 inhibits cardiomyocyte proliferation in mouse neonatal hearts by repressing CCND1 expression. Ann Transl Med 7. 10.21037/atm.2019.08.68.
- Grimm, D., Wehland, M., Pietsch, J., Aleshcheva, G., Wise, P., van Loon, J., Ulbrich, C., Magnusson, N., Infanger, M., and Bauer, J. (2014). Growing tissues in real and simulated microgravity: new methods for tissue engineering. Tissue Eng Part B, Reviews *20*. 10.1089/ten.TEB.2013.0704.
- Guo, Y., and Pu, W.T. (2020). Cardiomyocyte Maturation: New Phase in Development. Circ Res *126*, 1086-1106. 10.1161/CIRCRESAHA.119.315862.
- Hayashi, Y., Kuroda, T., Kishimoto, H., Wang, C., Iwama, A., and Kimura, K. (2014). Downregulation of rRNA transcription triggers cell differentiation. PloS One 9. 10.1371/journal.pone.0098586.
- Holaska, J., Rais-Bahrami, S., and Wilson, K. (2006). Lmo7 is an emerin-binding protein that regulates the transcription of emerin and many other muscle-relevant genes. Hum Mol Genet *15*. 10.1093/hmg/ddl423.
- Huang, P., Russell, A.L., Lefavor, R., Durand, N.C., James, E., Harvey, L., Zhang, C., Countryman, S., Stodieck, L., and Zubair, A.C. (2020). Feasibility, potency, and safety of growing human

- mesenchymal stem cells in space for clinical application. NPJ Microgravity *6*, 16. 10.1038/s41526-020-0106-z.
- Ingber, D. (1999). How cells (might) sense microgravity. FASEB J *13 Suppl*, S3-15. 10.1096/fasebj.13.9001.s3.
- Jha, R., Singh, M., Wu, Q., Gentillon, C., Preininger, M., and Xu, C. (2017). Downregulation of LGR5 Expression Inhibits Cardiomyocyte Differentiation and Potentiates Endothelial Differentiation from Human Pluripotent Stem Cells. Stem Cell Rep 9. 10.1016/j.stemcr.2017.07.006.
- Jha, R., Wile, B., Wu, Q., Morris, A.H., Maher, K.O., Wagner, M.B., Bao, G., and Xu, C. (2015). Molecular beacon-based detection and isolation of working-type cardiomyocytes derived from human pluripotent stem cells. Biomaterials *50*, 176-185. 10.1016/j.biomaterials.2015.01.043.
- Jha, R., Wu, Q., Singh, M., Preininger, M.K., Han, P., Ding, G., Cho, H.C., Jo, H., Maher, K.O., Wagner, M.B., and Xu, C. (2016). Simulated Microgravity and 3D Culture Enhance Induction, Viability, Proliferation and Differentiation of Cardiac Progenitors from Human Pluripotent Stem Cells. Sci Rep *6*, 30956. 10.1038/srep30956.
- Kawahara, Y., Manabe, T., Matsumoto, M., Kajiume, T., Matsumoto, M., and Yuge, L. (2009). LIF-free embryonic stem cell culture in simulated microgravity. PLoS One 4, e6343. 10.1371/journal.pone.0006343.
- Laflamme, M.A., Chen, K.Y., Naumova, A.V., Muskheli, V., Fugate, J.A., Dupras, S.K., Reinecke, H., Xu, C., Hassanipour, M., Police, S., et al. (2007). Cardiomyocytes derived from human embryonic stem cells in pro-survival factors enhance function of infarcted rat hearts. Nat Biotechnol *25*, 1015-1024.
- Laflamme, M.A., and Murry, C.E. (2005). Regenerating the heart. Nat Biotechnol 23, 845-856. 10.1038/nbt1117.
- Lan, F., Lee, A.S., Liang, P., Sanchez-Freire, V., Nguyen, P.K., Wang, L., Han, L., Yen, M., Wang, Y., Sun, N., et al. (2013). Abnormal calcium handling properties underlie familial hypertrophic cardiomyopathy pathology in patient-specific induced pluripotent stem cells. Cell Stem Cell *12*, 101-113. 10.1016/j.stem.2012.10.010.
- Lang, R., and Raffi, F. (2019). Dual-Specificity Phosphatases in Immunity and Infection: An Update. International journal of molecular sciences *20*. 10.3390/ijms20112710.
- Li, S., Ma, Z., Niu, Z., Qian, H., Xuan, D., Hou, R., and Ni, L. (2009). NASA-approved rotary bioreactor enhances proliferation and osteogenesis of human periodontal ligament stem cells. Stem Cells Dev *18*, 1273-1282. 10.1089/scd.2008.0371.
- Li, Y., Wang, L., Zhang, L., He, Z., Feng, G., Sun, H., Wang, J., Li, Z., Liu, C., Han, J., et al. (2019). Cyclin B3 is required for metaphase to anaphase transition in oocyte meiosis I. J Cell Biol *218*. 10.1083/jcb.201808088.
- Lian, X., Hsiao, C., Wilson, G., Zhu, K., Hazeltine, L.B., Azarin, S.M., Raval, K.K., Zhang, J., Kamp, T.J., and Palecek, S.P. (2012). Robust cardiomyocyte differentiation from human pluripotent stem cells via temporal modulation of canonical Wnt signaling. Proc Natl Acad Sci U S A *109*, E1848-1857. 10.1073/pnas.1200250109.
- Liu, R., Li, D., Sun, F., Rampoldi, A., Maxwell, J.T., Wu, R., Fischbach, P., Castellino, S.M., Du, Y., Fu, H., et al. (2020a). Melphalan induces cardiotoxicity through oxidative stress in cardiomyocytes derived from human induced pluripotent stem cells. Stem Cell Res Ther *11*, 470. 10.1186/s13287-020-01984-1.
- Liu, X., De la Cruz, E., Gu, X., Balint, L., Oxendine-Burns, M., Terrones, T., Ma, W., Kuo, H., Lantz, C., Bansal, T., et al. (2020b). Lymphoangiocrine signals promote cardiac growth and repair. Nature *588*. 10.1038/s41586-020-2998-x.
- Martinez, J., Dhawan, A., and Farach-Carson, M. (2018). Modular Proteoglycan Perlecan/ HSPG2: Mutations, Phenotypes, and Functions. Genes 9. 10.3390/genes9110556.
- Meisenberg, C., Tait, P., Dianova, I., Wright, K., Edelmann, M., Ternette, N., Tasaki, T., Kessler, B., Parsons, J., Kwon, Y., and Dianov, G. (2012). Ubiquitin ligase UBR3 regulates cellular levels of the essential DNA repair protein APE1 and is required for genome stability. Nucleic Acids Res *40*. 10.1093/nar/gkr744.
- Moscu-Gregor, A., Marschall, C., Müntjes, C., Schönecker, A., Schuessler-Hahn, F., Hohendanner, F., Parwani, A., Boldt, L., Ott, C., Bennewiz, A., et al. (2020). Novel variants in TECRL cause

- recessive inherited CPVT type 3 with severe and variable clinical symptoms. J Cardiovasc Electrophysiol *31*. 10.1111/jce.14446.
- Nguyen, D., Hookway, T., Wu, Q., Jha, R., Preininger, M., Chen, X., Easley, C., Spearman, P., Deshpande, S., Maher, K., et al. (2014). Microscale generation of cardiospheres promotes robust enrichment of cardiomyocytes derived from human pluripotent stem cells. Stem Cell Rep 3. 10.1016/j.stemcr.2014.06.002.
- Pöss, J., Ukena, C., Kindermann, I., Ehrlich, P., Fuernau, G., Ewen, S., Mahfoud, F., Kriechbaum, S., Böhm, M., and Link, A. (2015). Angiopoietin-2 and outcome in patients with acute decompensated heart failure. Clin Res Cardiol *104*. 10.1007/s00392-014-0787-y.
- Preininger, M.K., Jha, R., Maxwell, J.T., Wu, Q., Singh, M., Wang, B., Dalal, A., McEachin, Z.T., Rossoll, W., Hales, C.M., et al. (2016). A human pluripotent stem cell model of catecholaminergic polymorphic ventricular tachycardia recapitulates patient-specific drug responses. Dis Model Mech *9*, 927-939. 10.1242/dmm.026823.
- Pyo, R., Sui, J., Dhume, A., Palomeque, J., Blaxall, B., Diaz, G., Tunstead, J., Logothetis, D., Hajjar, R., and Schecter, A. (2006). CXCR4 modulates contractility in adult cardiac myocytes. J Mol Cell Cardiol *41*. 10.1016/j.yjmcc.2006.08.008.
- Rampoldi, A., Jha, R., Fite, J., Boland, G., and Xu, C. (2021). Cryopreservation and CO2-independent culture of 3D cardiac progenitors for spaceflight experiments. Biomaterials *269*, 120673. 10.1016/j.biomaterials.2021.120673.
- Ribeiro, I., Kawakami, Y., Büscher, D., Raya, A., Rodríguez-León, J., Morita, M., Rodríguez Esteban, C., and Izpisúa Belmonte, J. (2007). Tbx2 and Tbx3 regulate the dynamics of cell proliferation during heart remodeling. PloS One 2. 10.1371/journal.pone.0000398.
- Ribeiro, M., Tertoolen, L., Guadix, J., Bellin, M., Kosmidis, G., D'Aniello, C., Monshouwer-Kloots, J., Goumans, M., Wang, Y., Feinberg, A., et al. (2015). Functional maturation of human pluripotent stem cell derived cardiomyocytes in vitro--correlation between contraction force and electrophysiology. Biomaterials *51*. 10.1016/j.biomaterials.2015.01.067.
- Saraf, A., Rampoldi, A., Chao, M., Li, D., Armand, L., Hwang, H., Liu, R., Jha, R., Fu, H., Maxwell, J.T., and Xu, C. (2021). Functional and molecular effects of TNF-alpha on human iPSC-derived cardiomyocytes. Stem Cell Res *52*, 102218. 10.1016/j.scr.2021.102218.
- Scholz, A., Plate, K., and Reiss, Y. (2015). Angiopoietin-2: a multifaceted cytokine that functions in both angiogenesis and inflammation. Ann N Y Acad Sci 1347. 10.1111/nyas.12726.
- Sharma, A., Clemens, R.A., Garcia, O., Taylor, D.L., Wagner, N.L., Shepard, K.A., Gupta, A., Malany, S., Grodzinsky, A.J., Kearns-Jonker, M., et al. (2022). Biomanufacturing in low Earth orbit for regenerative medicine. Stem Cell Rep *17*, 1-13. 10.1016/j.stemcr.2021.12.001.
- Shen, H., Gan, P., Wang, K., Darehzereshki, A., Wang, K., Kumar, S., Lien, C., Patterson, M., Tao, G., and Sucov, H. (2020). Mononuclear diploid cardiomyocytes support neonatal mouse heart regeneration in response to paracrine IGF2 signaling. eLife 9. 10.7554/eLife.53071.
- Simone, T., Higgins, C., Czekay, R., Law, B., Higgins, S., Archambeault, J., Kutz, S., and Higgins, P. (2014). SERPINE1: A Molecular Switch in the Proliferation-Migration Dichotomy in Wound-"Activated" Keratinocytes. Adv Wound Care 3. 10.1089/wound.2013.0512.
- Tamargo, J., Caballero, R., Gómez, R., Valenzuela, C., and Delpón, E. (2004). Pharmacology of cardiac potassium channels. Cardio Res 62. 10.1016/j.cardiores.2003.12.026.
- Tao, G., Levay, A., Peacock, J., Huk, D., Both, S., Purcell, N., Pinto, J., Galantowicz, M., Koch, M., Lucchesi, P., et al. (2012). Collagen XIV is important for growth and structural integrity of the myocardium. Journal of molecular and cellular cardiology *53*. 10.1016/j.yjmcc.2012.08.002.
- Unsworth, B., and Lelkes, P. (1998). Growing tissues in microgravity. Nat Med 4. 10.1038/nm0898-901
- Wnorowski, A., Sharma, A., Chen, H., Wu, H., Shao, N., Sayed, N., Liu, C., Countryman, S., Stodieck, L., Rubins, K., et al. (2019). Effects of Spaceflight on Human Induced Pluripotent Stem Cell-Derived Cardiomyocyte Structure and Function. Stem Cell Rep *13*. 10.1016/j.stemcr.2019.10.006.
- Yuge, L., Kajiume, T., Tahara, H., Kawahara, Y., Umeda, C., Yoshimoto, R., Wu, S., Yamaoka, K., Asashima, M., Kataoka, K., and Ide, T. (2006). Microgravity potentiates stem cell proliferation while sustaining the capability of differentiation. Stem Cells Dev *15*. 10.1089/scd.2006.15.921.

- Zhang, S., Liu, P., Chen, L., Wang, Y., Wang, Z., and Zhang, B. (2015). The effects of spheroid formation of adipose-derived stem cells in a microgravity bioreactor on stemness properties and therapeutic potential. Biomaterials *41*, 15-25. 10.1016/j.biomaterials.2014.11.019.
- Zhang, S., Zhang, Y., Chen, L., Liu, T., Li, Y., Wang, Y., and Geng, Y. (2013). Efficient large-scale generation of functional hepatocytes from mouse embryonic stem cells grown in a rotating bioreactor with exogenous growth factors and hormones. Stem Cell Res Ther *4*. 10.1186/scrt356.
- Zhu, W., Zhao, M., Mattapally, S., Chen, S., and Zhang, J. (2018). CCND2 Overexpression Enhances the Regenerative Potency of Human Induced Pluripotent Stem Cell-Derived Cardiomyocytes: Remuscularization of Injured Ventricle. Circ Res *122*, 88-96. 10.1161/CIRCRESAHA.117.311504.

FIGURE LEGENDS

Figure 1. Spaceflight experimental design.

- (A) Schematic of spaceflight operational plan. Scale bar = 200µm.
- (B) Schematic of MVP sample collection plan.
- (C) Schematic of MVP system.

ICC, immunocytochemistry; MVP, the Multi-specimen Variable-gravity Platform. See also Figure S1.

Figure 2. Space microgravity increases cardiac sphere size and improves proliferation of enriched hiPSC-CMs.

- (A) Cell morphology of cardiac spheres derived from SCVI-273 and IMR90 hiPSCs from ISS cultures post-flight (Scale bar = 200μm).
- (B) Diameters of cardiac spheres derived from SCVI-273 and IMR90 hiPSCs (n=72-180 spheres).
- (C) Immunocytochemistry analysis of IMR90 cultures to detect cardiomyocyte purity by cardiac marker NKX2.5 (red) and proliferation by Ki-67 (green) and cardiac marker cTNI (red) (Scale bar = 50µm).
- (D) Percentage of NKX2.5-positive cells and Ki-67-positive cells in IMR90 cultures. Aliquots of ISS cultures post-flight were dissociated, replated, and subjected to immunocytochemistry (n=3 cultures).
- (E) Expression of genes associated with proliferation in IMR90 cultures (3 weeks on the ISS) and SCVI-273 cultures (3 days on the ISS) (n = 3 cultures).
- (F) Counts of nuclei in samples from IMR90 cultures (n = 6 wells) after the cells were dissociated, replated and stained.

Statistical analyses was performed with unpaired, two-tailed Student's t test for B, D and F, and one-way ANOVA for E. *, P < 0.05; **, P < 0.01; ***, P < 0.001; and ****, P < 0.0001. Data are presented as mean \pm standard deviation. ISS 1G, the 1G condition on the International Space Station; ISS μ G, the microgravity condition on the International Space Station.

Figure 3. Space microgravity cultures generated enriched cardiomyocytes with increased cell size.

- (A) Immunocytochemical analysis of cardiac proteins in IMR90 cells from ISS cultures post-flight, including cTNT (red); pan-cadherin (red); α -actinin (green) and NKX2.5 (red) (Scale bar = 50 μ m).
- (B) Comparison of cellular parameters of IMR90 hiPSC-CMs.

on the ISS) (n=3 cultures).

Statistical analyses was performed with unpaired, two-tailed Student's t test. **, P < 0.01, and ****, P < 0.0001. Data are presented as mean \pm standard deviation (ISS 1G n=53 cells; ISS μ G n=73 cells). ISS 1G, the 1G condition on the International Space Station; ISS μ G, the microgravity condition on the International Space Station.

Figure 4. Space microgravity improves cardiac structure of hiPSC-CMs.

(A) Structural analysis of IMR90 hiPSC-CMs from ISS cultures post-flight. Cells were dissociated, replated and stained for sarcomeric α-actinin (green) and Hoechst (blue). Overall appearance of myofibrillar structure was categorized into 3 different levels and percentage of the cells by the scores was generated by counting n=53 cells from ISS 1G and n=73 cells from ISS μG cultures.

(B) qRT-PCR panel showing relative mRNA expression levels of gene associated with cardiac

structure in cells derived from IMR90 hiPSCs (3 weeks on the ISS) and SCVI-273 hiPSCs (3 days

Statistical analyses was performed with one-way ANOVA. *, P < 0.05; **, P < 0.01; ***, P < 0.001; and ****, P < 0.0001. Data are presented as mean ± standard deviation (n=3 cultures). ISS 1G, the 1G condition on the International Space Station; ISS μ G, the microgravity condition on the International Space Station.

Figure 5. Space microgravity improves intracellular Ca²⁺ handling in hiPSC-CMs.

- (A) Representative traces of normal Ca²⁺ transients or abnormal Ca²⁺ transients of IMR90 hiPSC-CMs from ISS cultures post-flight.
- (B) Pie chart showing the percentage of cells exhibiting normal Ca²⁺ transients or abnormal Ca²⁺ transients (ISS 1G n=36 cells; ISS µG n=81 cells).

- (C) Ca^{2+} transient analyses with parameters presented as mean \pm standard deviation (ISS 1G n=28 cells; ISS μ G n=75 cells).
- (D) qRT-PCR panel showing relative mRNA expression levels of genes associated with Ca²⁺ handling in cells derived from IMR90 hiPSCs (3 weeks on the ISS) and SCVI-273 hiPSCs (3 days on the ISS) (n=3 cultures).

Statistical analyses was performed with unpaired, two-tailed Student's t test for C and one-way ANOVA for D. ***, P < 0.001 and ****, P < 0.0001. ISS 1G, the 1G condition on the International Space Station; ISS μ G, the microgravity condition on the International Space Station.

Figure 6. Differentially expressed genes and gene ontology (GO) terms identified by RNA-sequencing analysis of hiPSC-CMs exposed to space microgravity.

- (A) Volcano plot illustrating differentially expressed genes between ISS μ G and ISS 1G samples (n=3 cultures) collected from SCVI-273 cultures of 3 days on the ISS (short-term exposure to microgravity).
- (B) Dot plot showing up- and downregulated GO terms of biological processes.

GSEA, Gene Set Enrichment Analysis; ISS 1G, the 1G condition on the International Space Station; ISS μ G, the microgravity condition on the International Space Station. See also Figures S2-7.

Figure 7. Chord diagrams showing the relationship between gene ontology (GO) terms and differentially expressed genes in hiPSC-CMs exposed to space microgravity.

- (A) Chord diagram of selected upregulated GO terms and genes in ISS μ G vs. ISS 1G of SCVI-273 cultures of 3 day on the ISS.
- (B) Chord diagram of selected downregulated GO terms and genes.
- GO terms were presented on the right, genes on the left, colored squares on the left indicated log₂(fold change) value from highest to lowest (n=3 cultures).

Figure 1

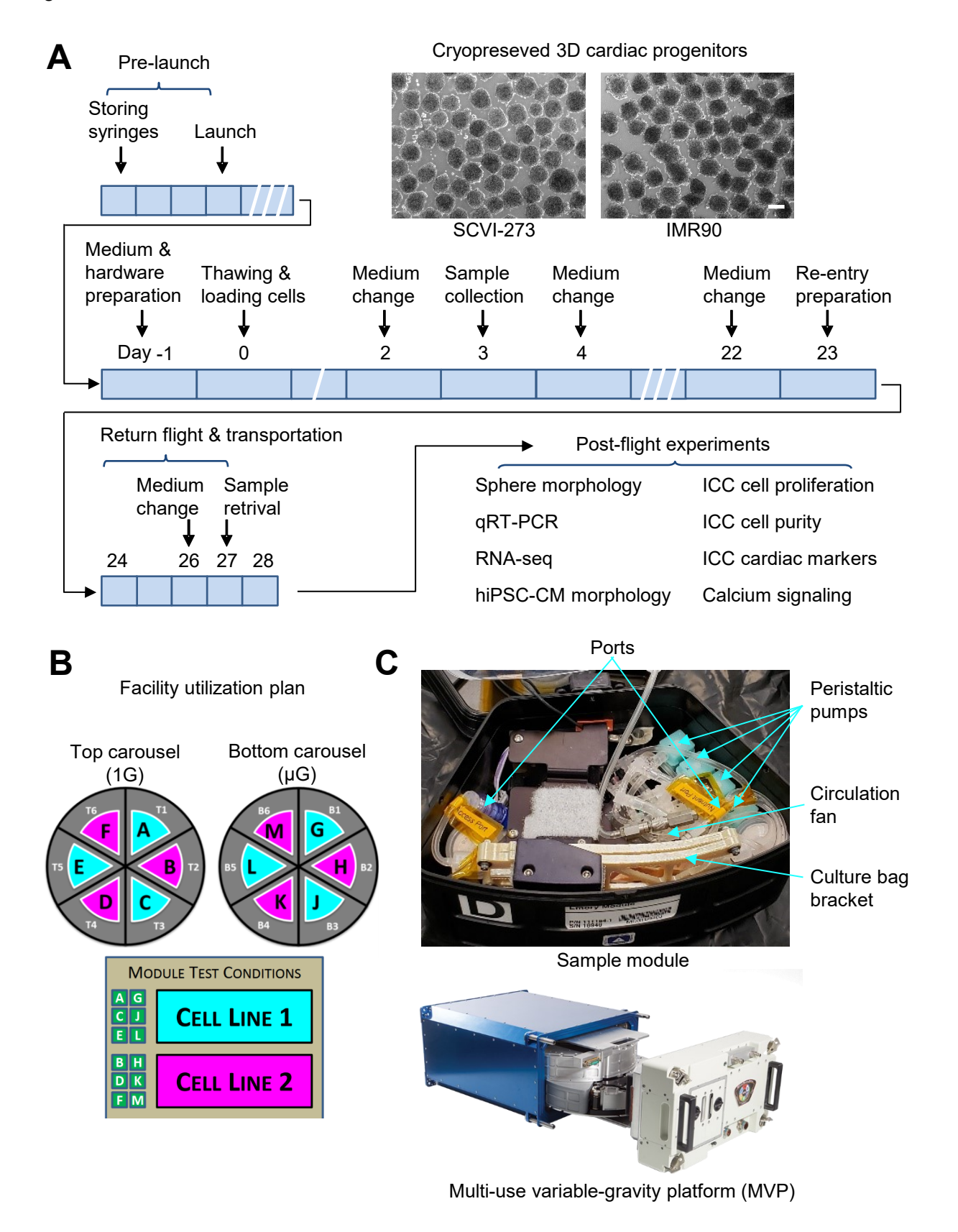


Figure 2

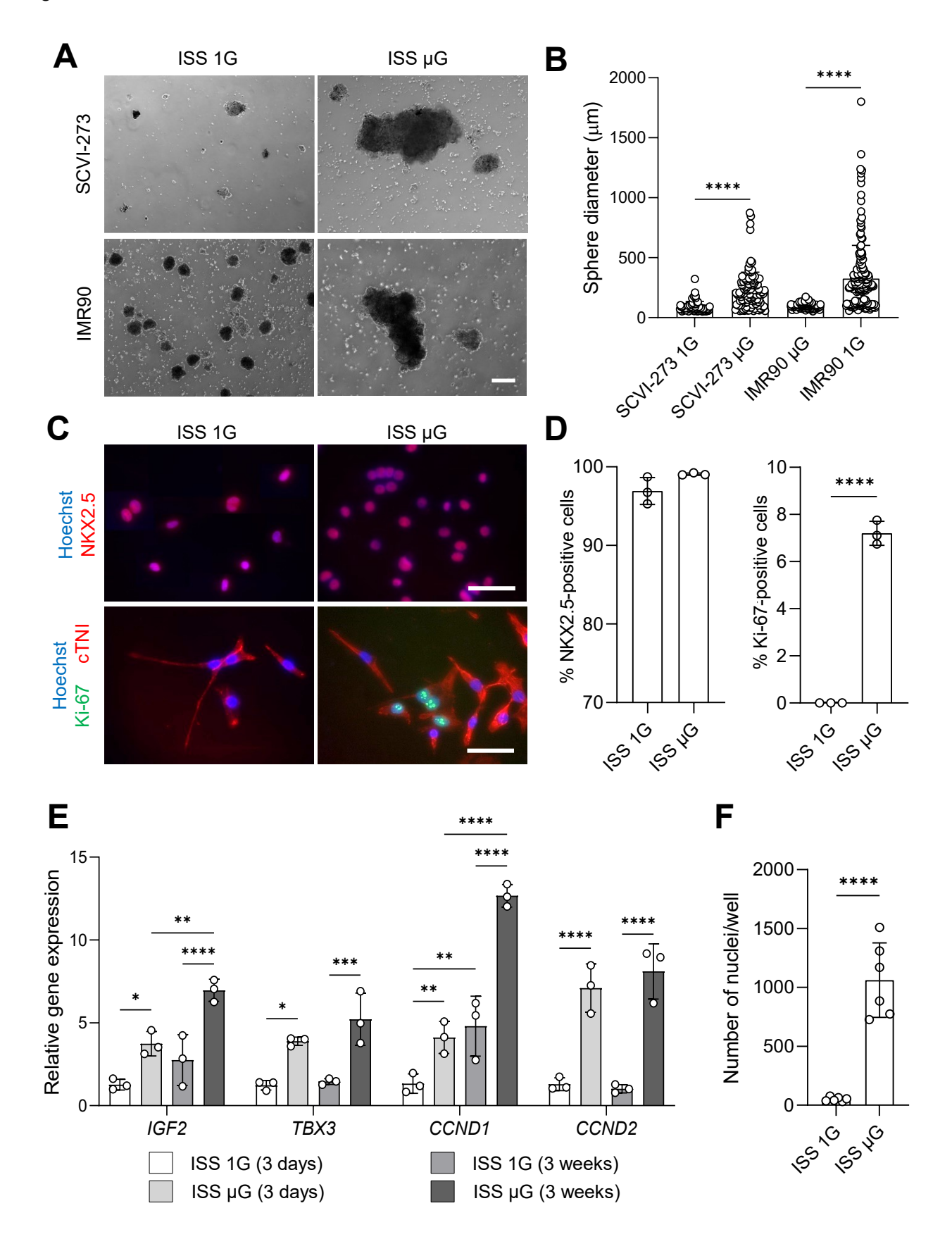


Figure 3

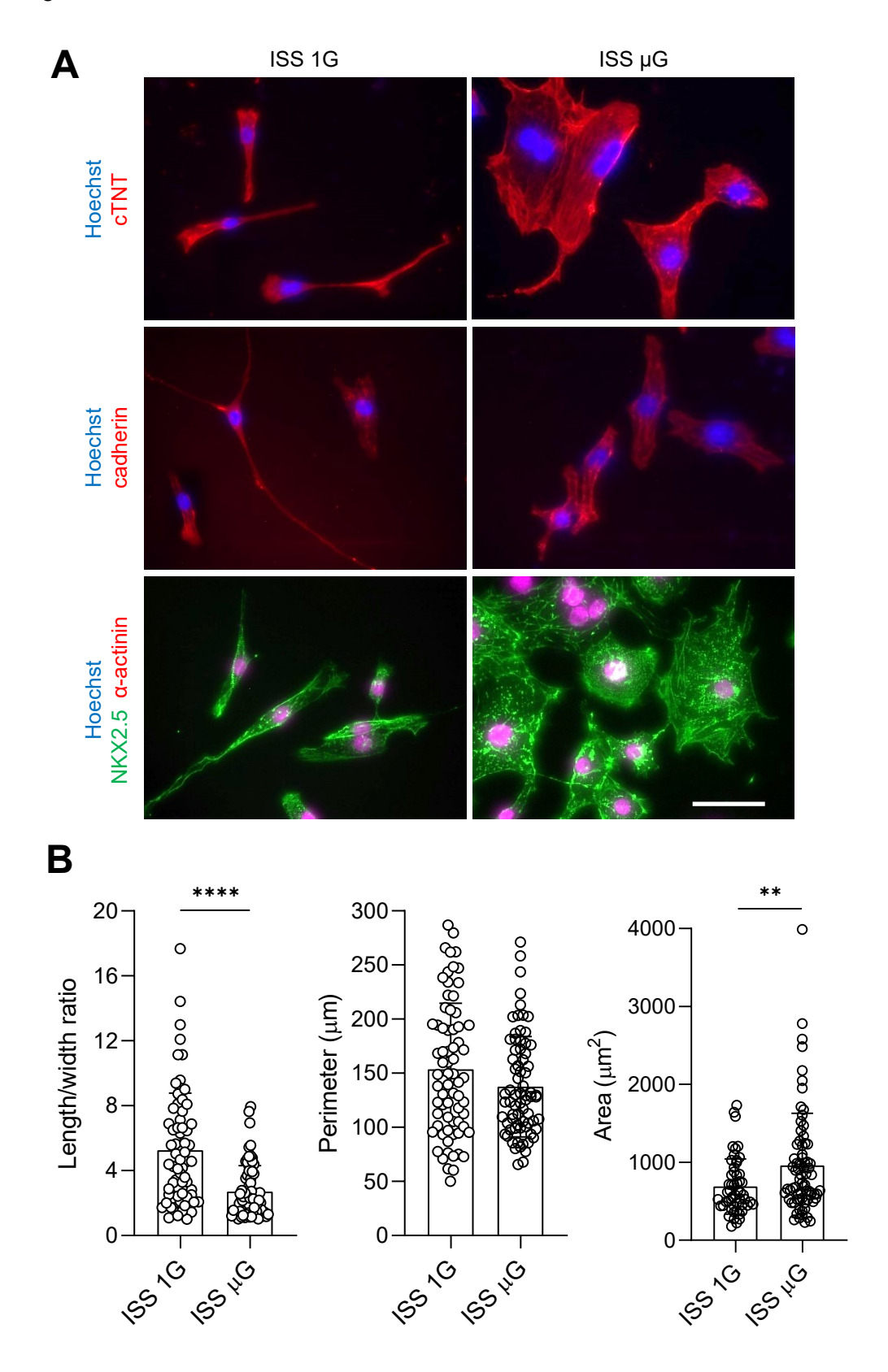
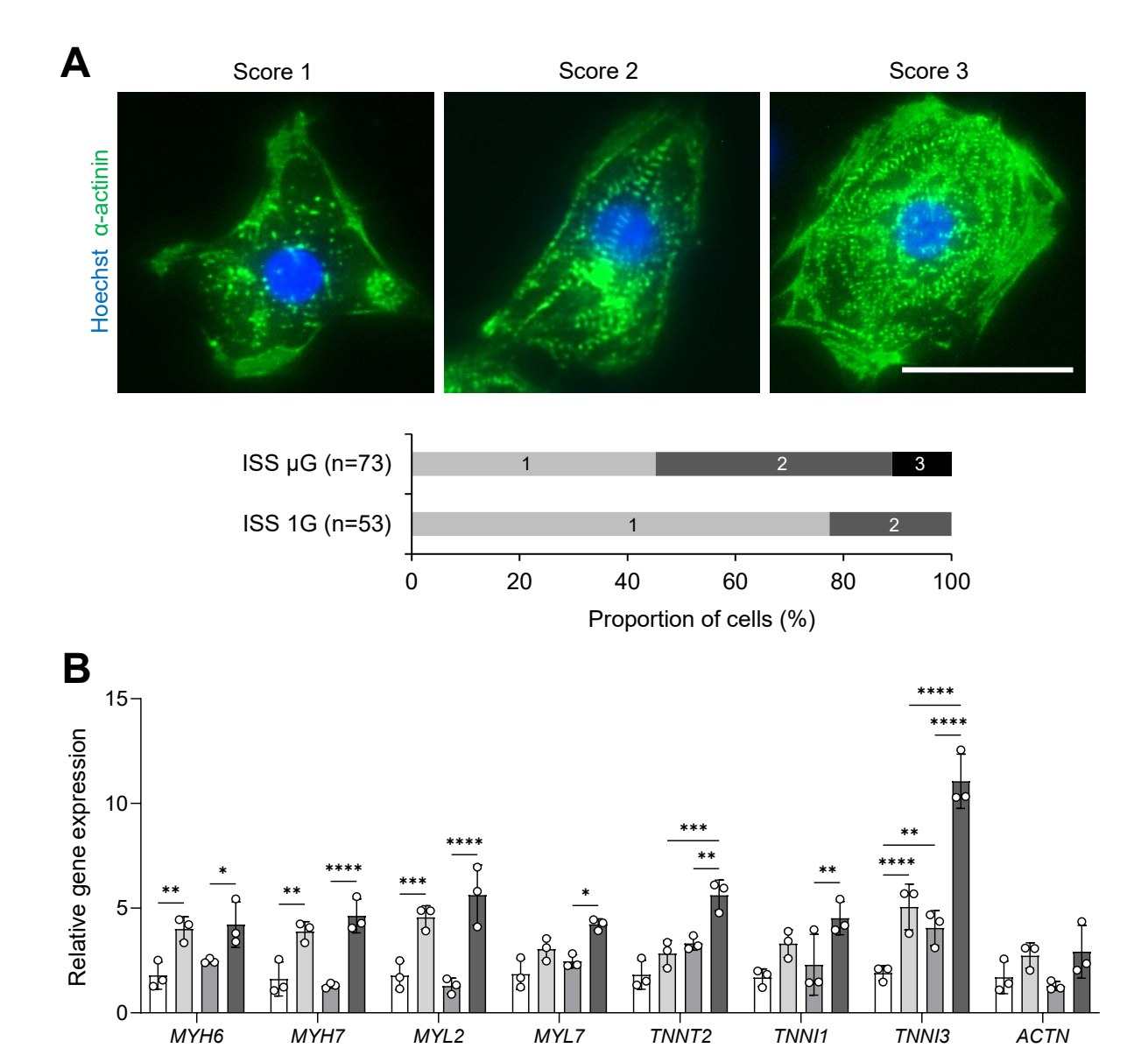


Figure 4

ISS 1G (3 days)



ISS μG (3 days)

ISS 1G (3 weeks)

ISS µG (3 weeks)

Figure 5

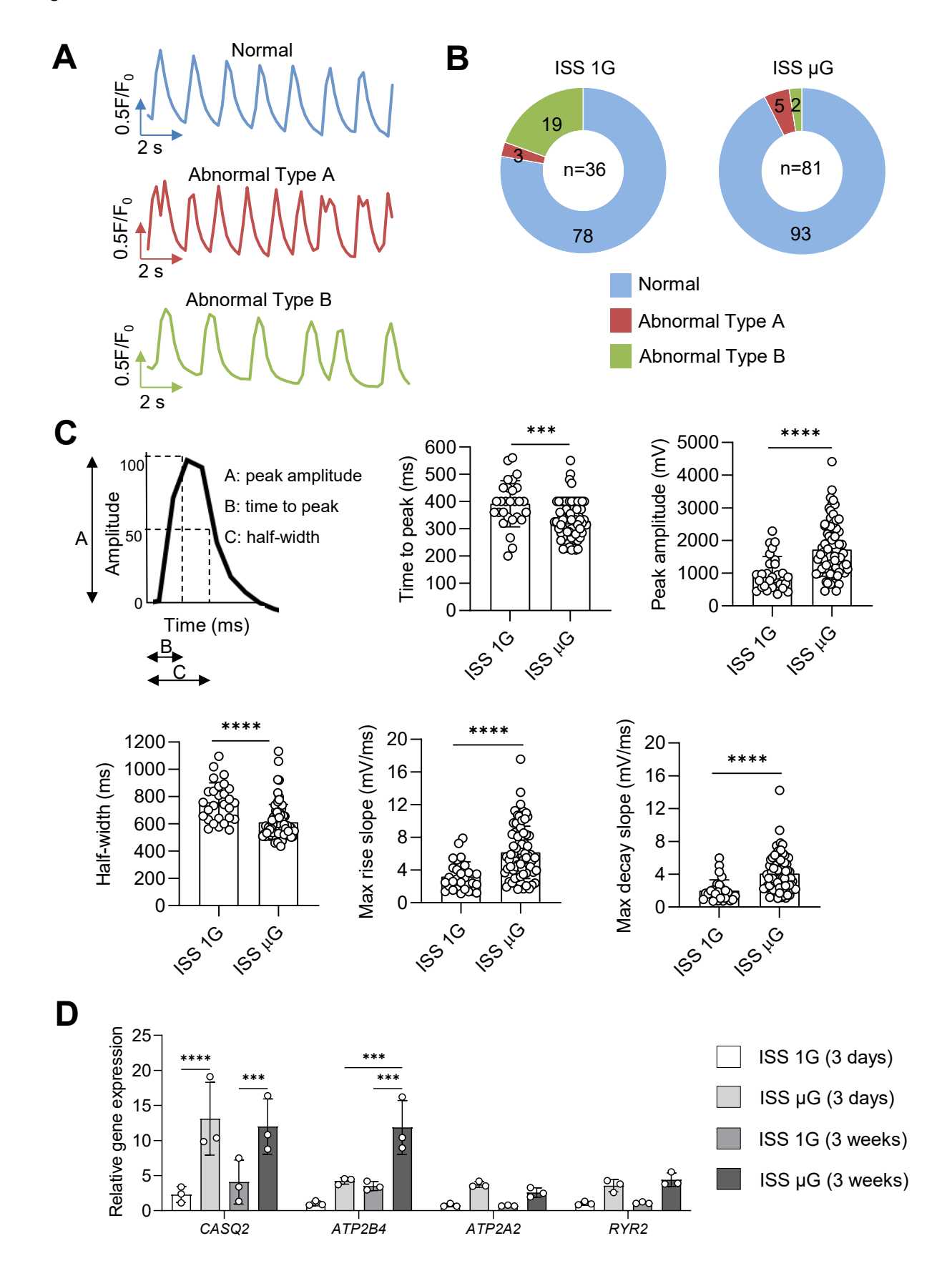
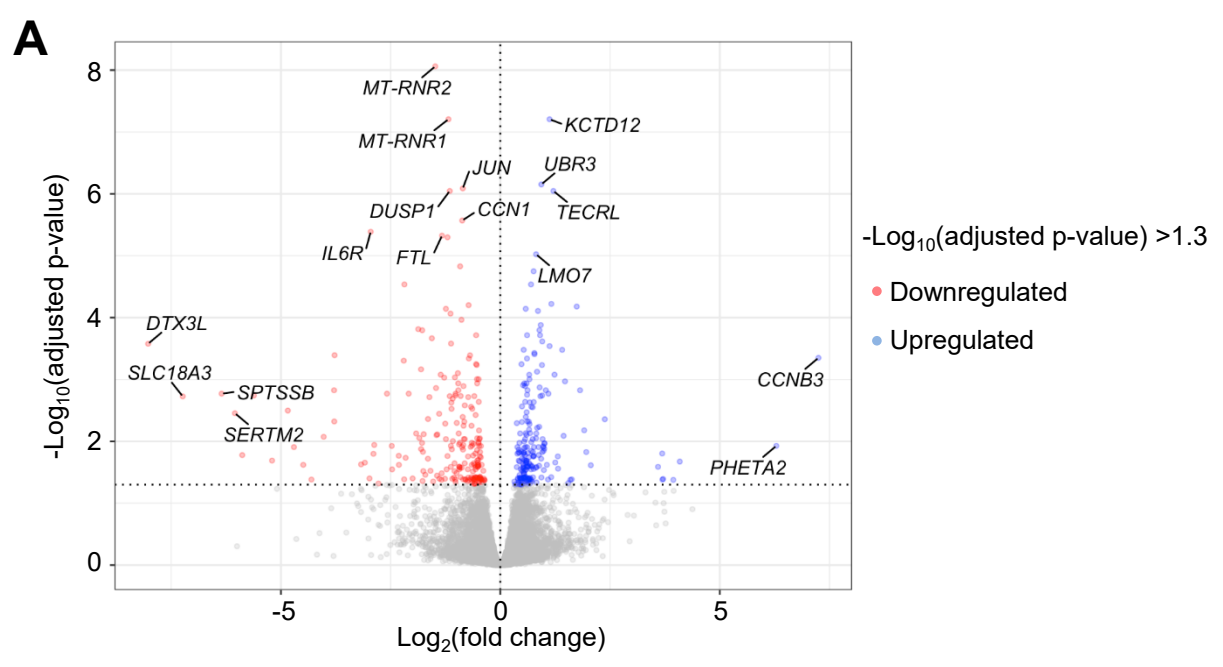


Figure 6



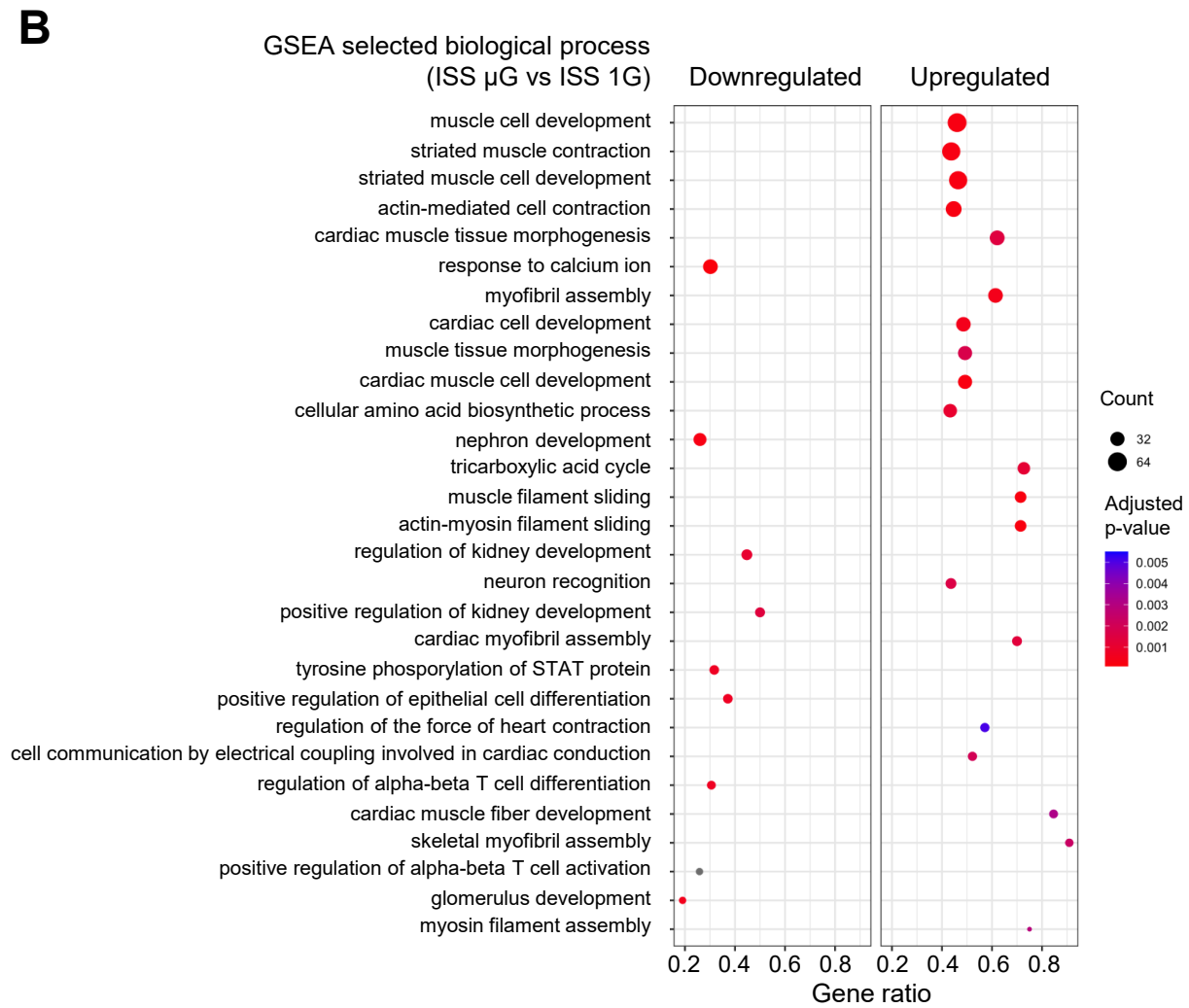
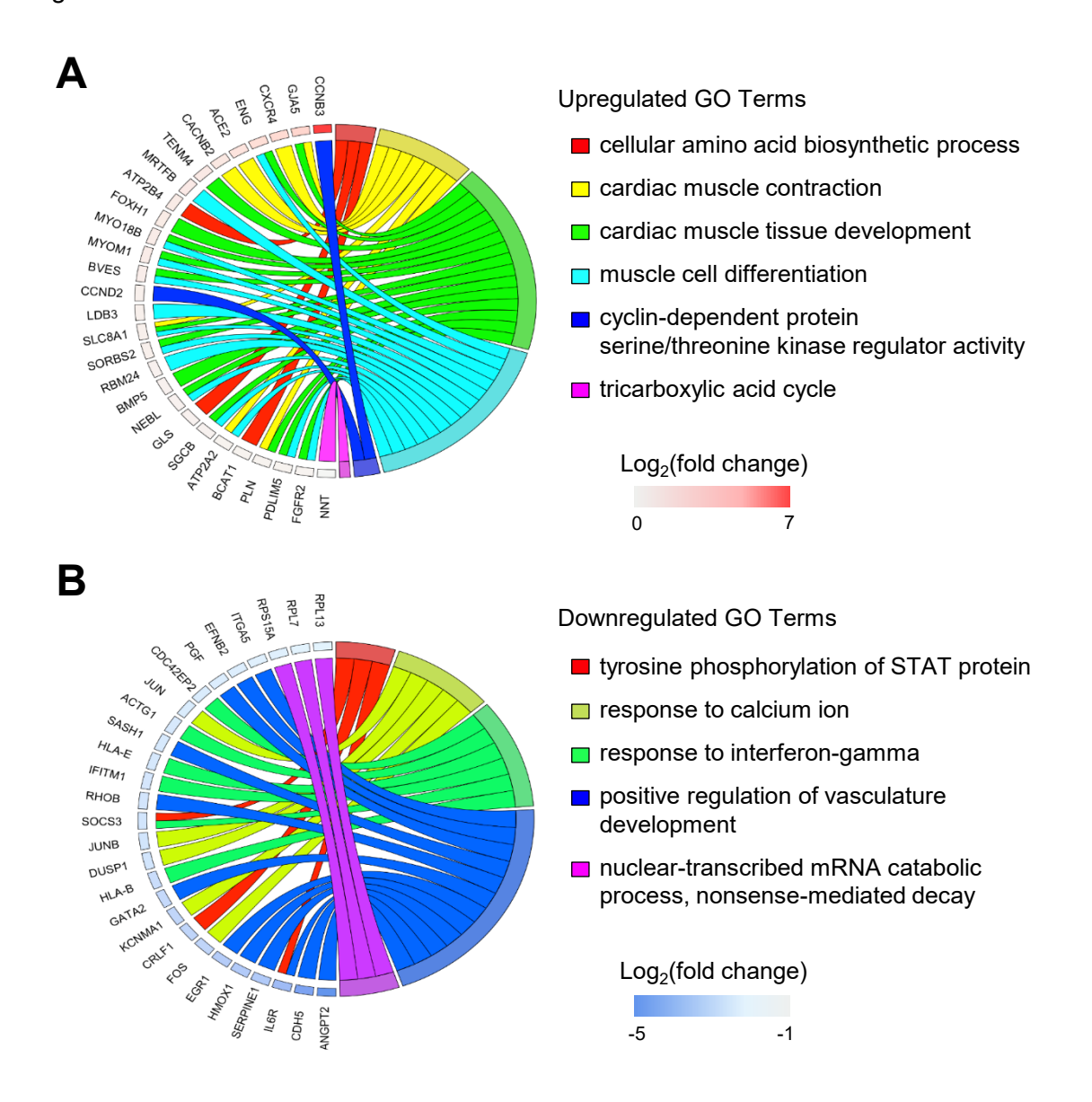
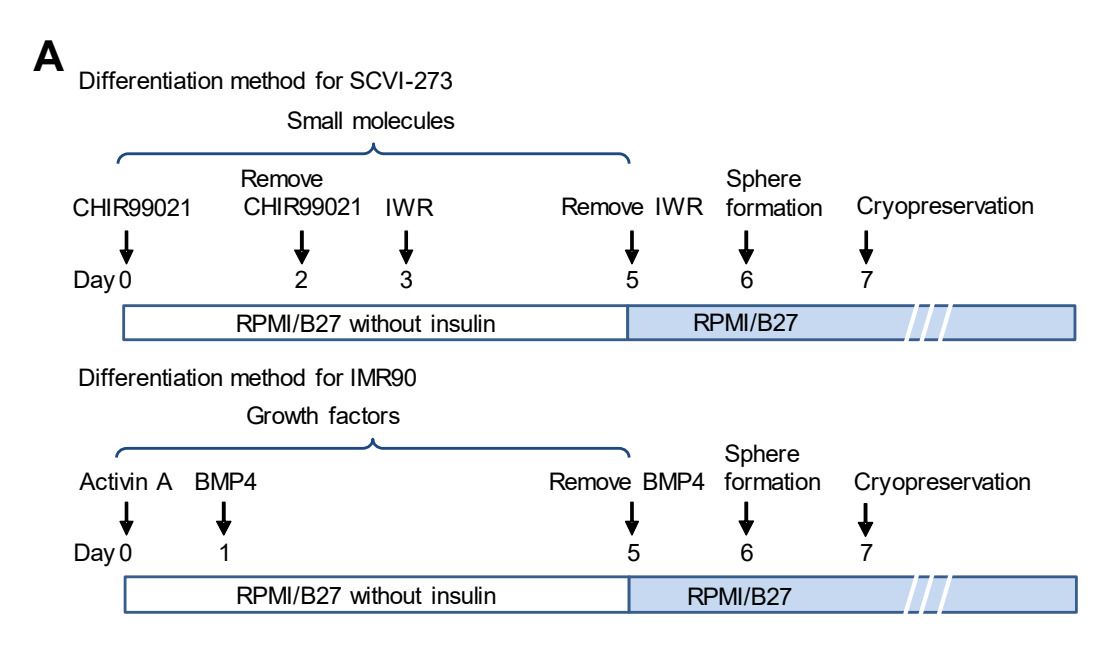


Figure 7



Supplemental Information



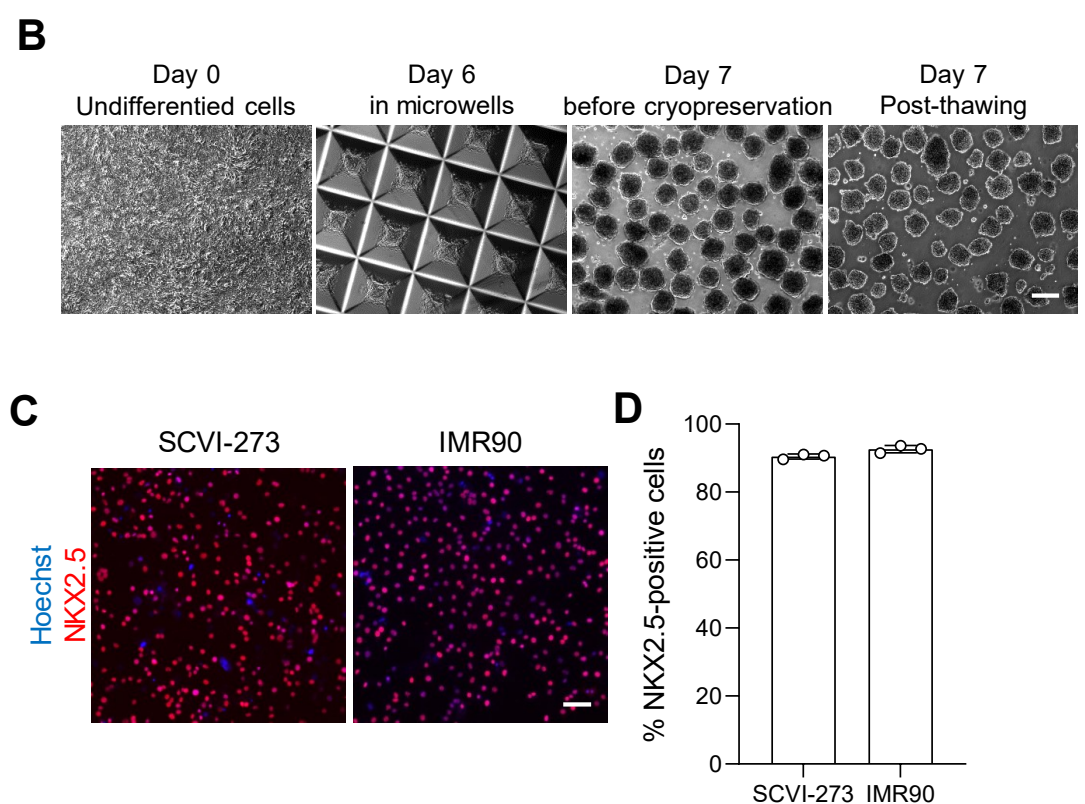
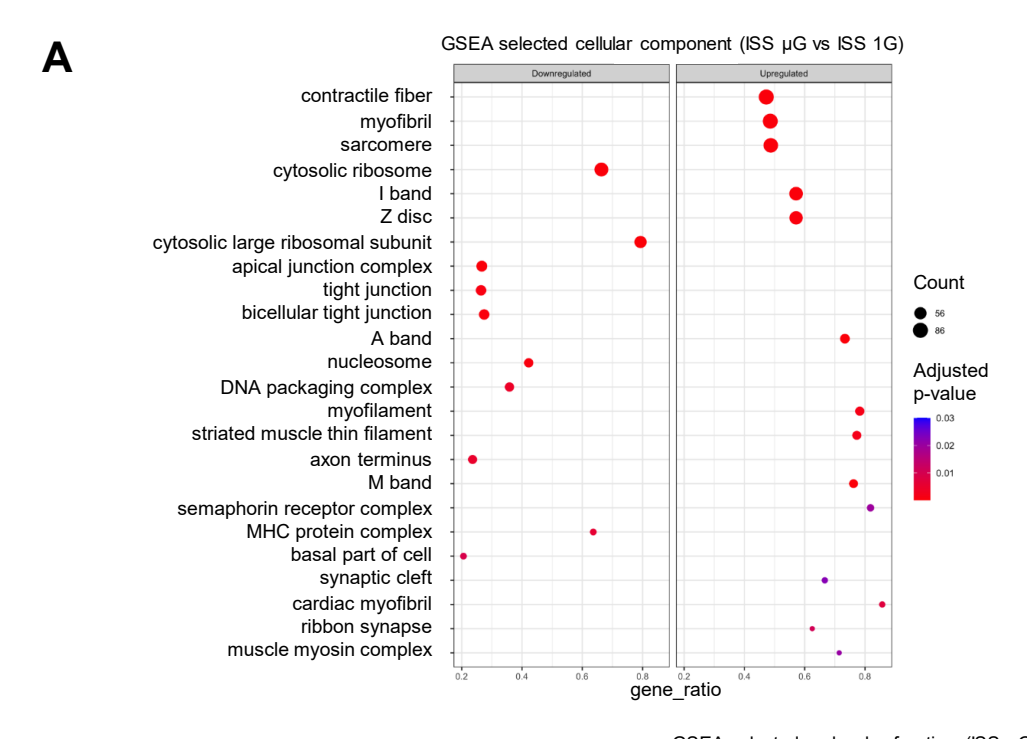


Figure S1. Directed differentiation of hiPSCs and 3D culture of cardiac spheres generate enriched cardiomyocytes, related to Figure 1. (A) Schematic of cardiomyocyte differentiation from hiPSCs. (B) Representative images of stem cells and cardiac spheres (Scale bar = $200\mu m$). (C) Representative images of NKX2.5-positive cells in pre-testing of cell preparations derived from IMR90 and SCVI-273 hiPSCs for the ISS experiment. (Scale bar = $100\mu m$). (D) Pre-testing purity of cardiomyocytes derived from IMR90 and SCVI-273 hiPSCs analyzed by ArrayScan (n = 3 cultures). Data are presented as mean \pm standard deviation.



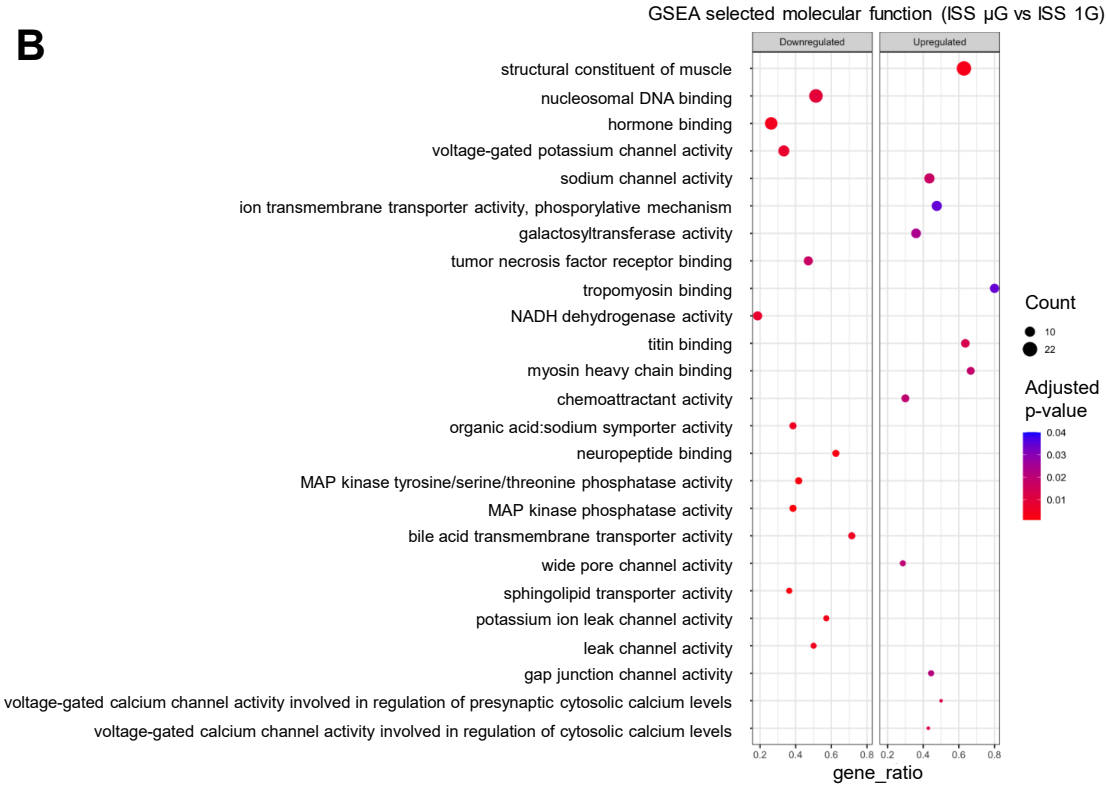
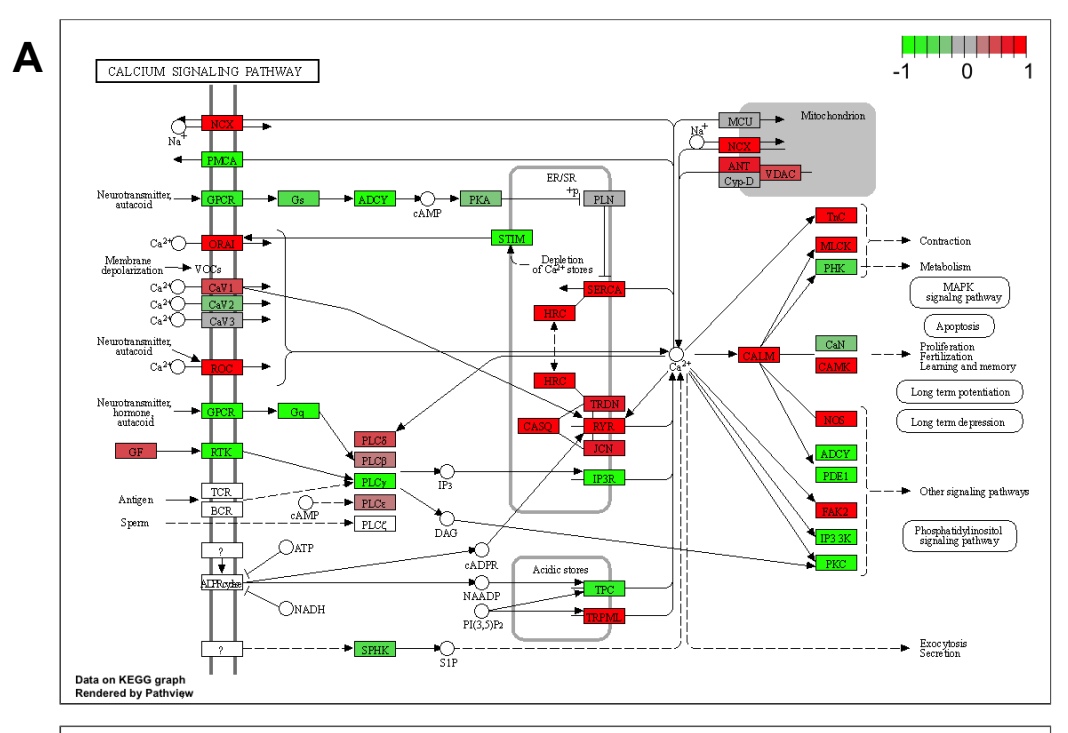


Figure S2. GO terms identified by RNA-seq analysis of SCVI-273 cardiac spheres exposed to space microgravity, related to Figure 6. (A) Dot plot showing upregulated and downregulated genes clustered by GO enrichment analysis of cellular component from ISS μ G and ISS 1G samples (n=3 cultures) collected 3 day after thawing onboard ISS (short-term exposure to microgravity). (B) Dot plot showing upand downregulated genes clustered by GO enrichment analysis of molecular function. GSEA, Gene Set Enrichment Analysis; ISS 1G, the 1G condition on the International Space Station; ISS μ G, the microgravity condition on the International Space Station.



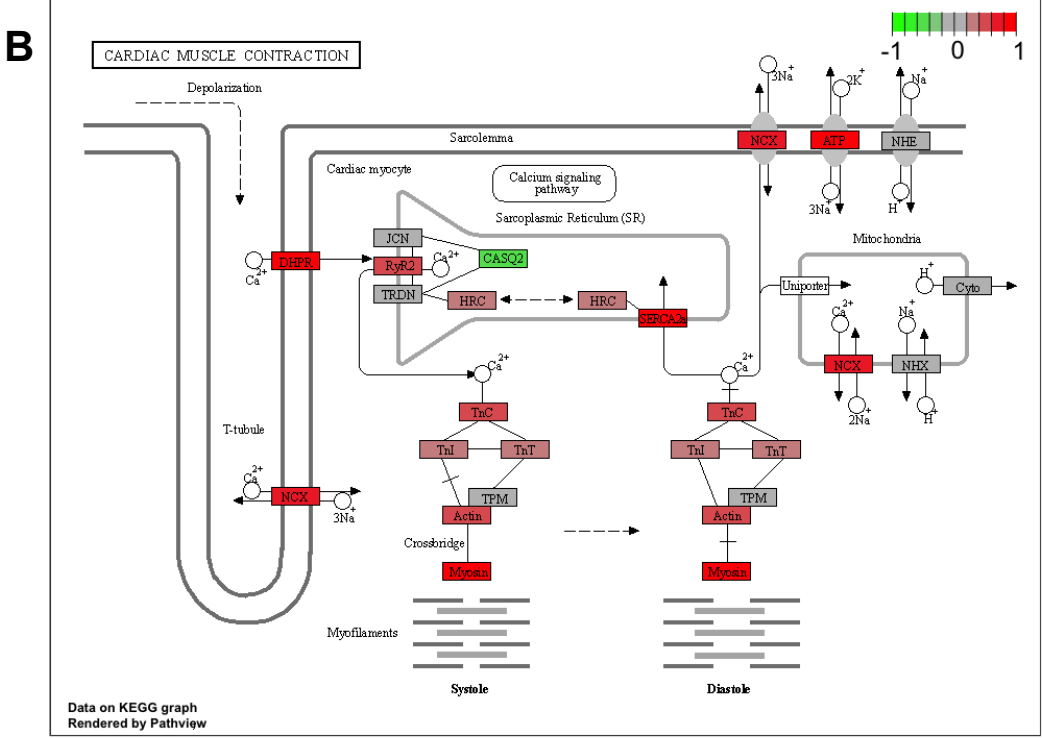


Figure S3. KEGG pathway of calcium signaling in SCVI-273 cardiac spheres after 3 days in the ISS μ G condition compared with the ISS 1G condition, related to Figure 6. (A) Upregulation of calcium signaling in IMR90 hiPSC-CMs after 3 days in the ISS μ G condition compared with the ISS 1G condition. (B) Upregulation of cardiac muscle contraction in IMR90 hiPSC-CMs after 3 days in the ISS μ G condition compared with the ISS 1G condition. KEGG, Kyoto Encyclopedia of Genes and Genomes. ISS 1G, the 1G condition on the International Space Station; ISS μ G, the microgravity condition on the International Space Station.

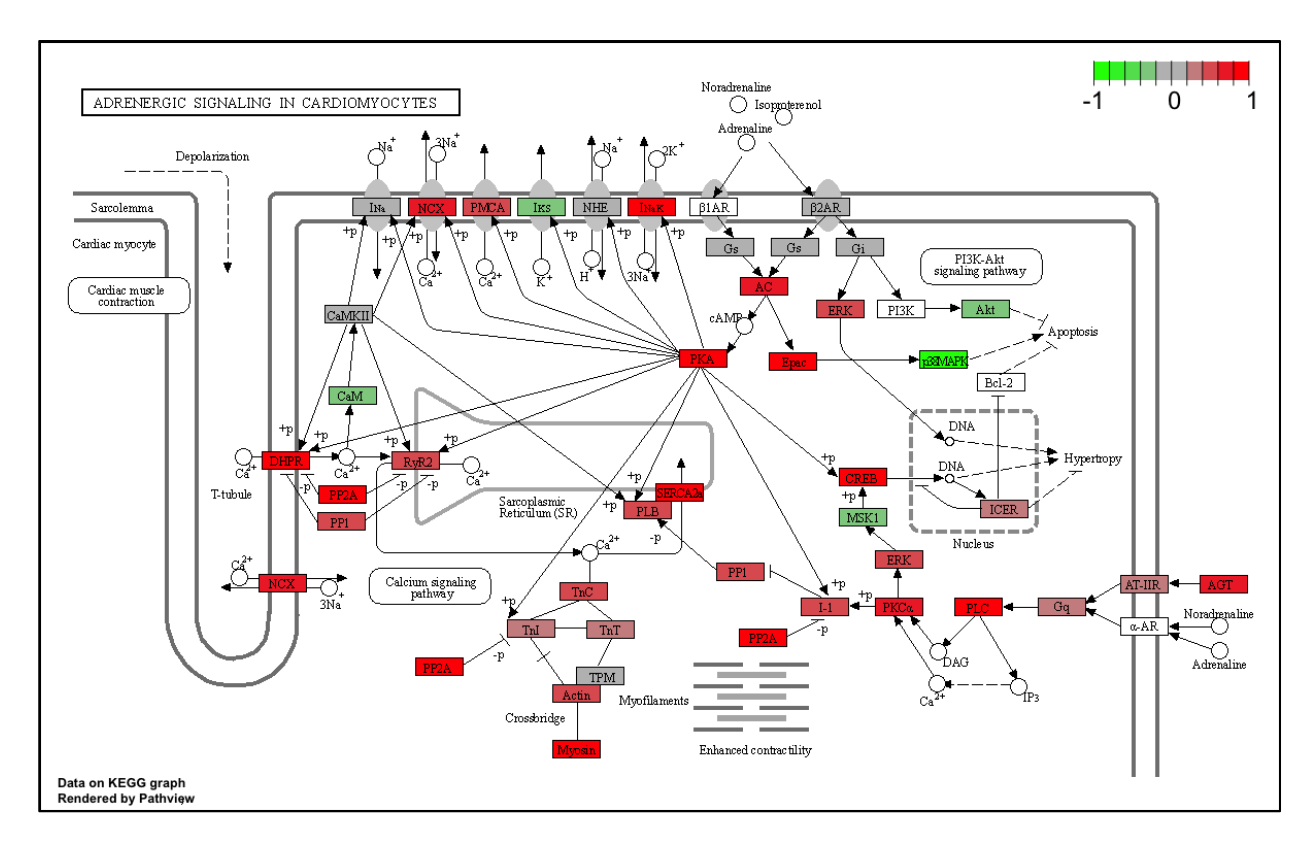


Figure S4. Upregulation of KEGG pathway of adrenergic signaling in SCVI-273 cardiac spheres after 3 days in the ISS μ G condition compared with the ISS 1G condition, related to Figure 6. KEGG, Kyoto Encyclopedia of Genes and Genomes. ISS 1G, the 1G condition on the International Space Station; ISS μ G, the microgravity condition on the International Space Station.

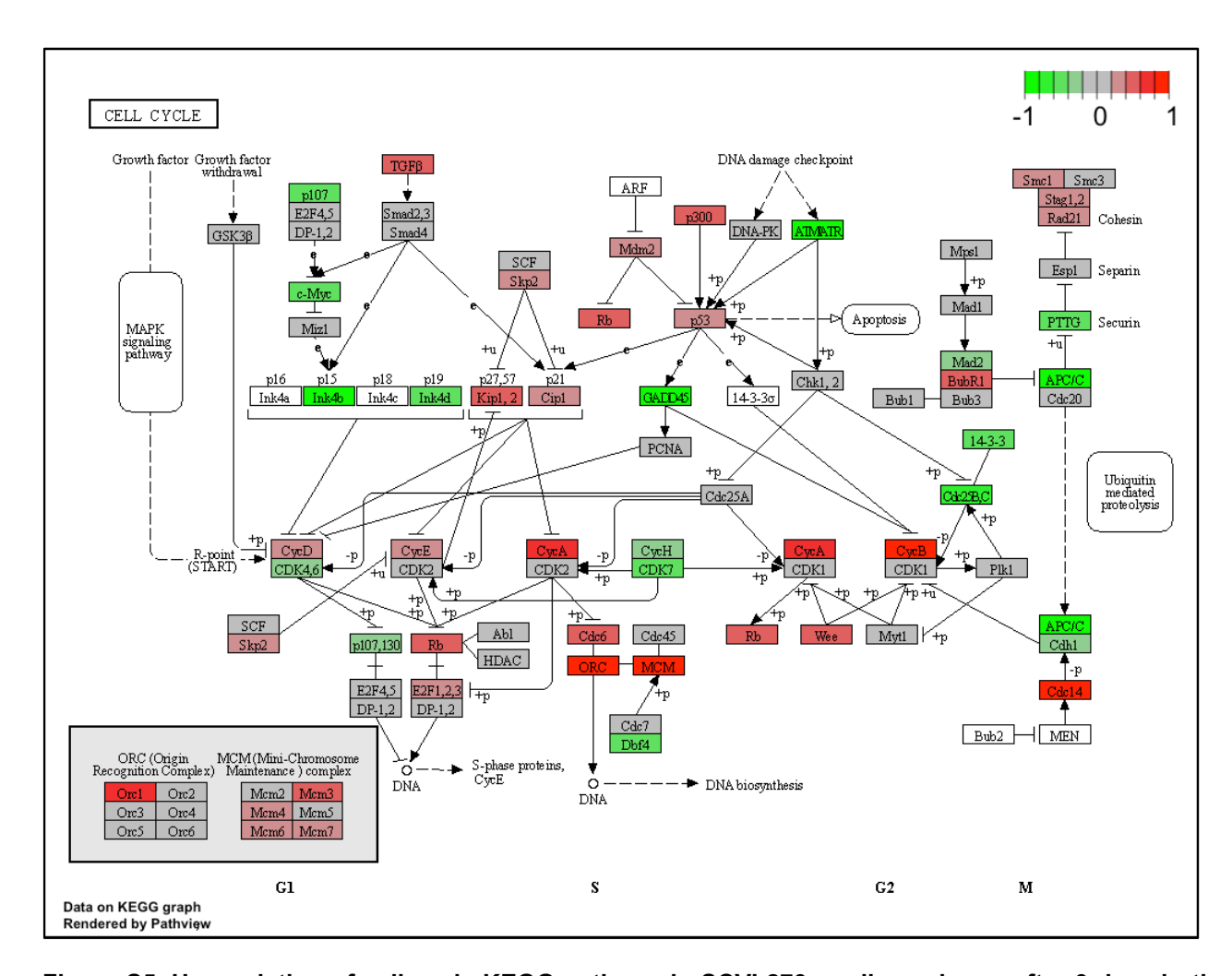


Figure S5. Upregulation of cell cycle KEGG pathway in SCVI-273 cardiac spheres after 3 days in the ISS μ G condition compared with the ISS 1G condition, related to Figure 6. KEGG, Kyoto Encyclopedia of Genes and Genomes. ISS 1G, the 1G condition on the International Space Station; ISS μ G, the microgravity condition on the International Space Station.

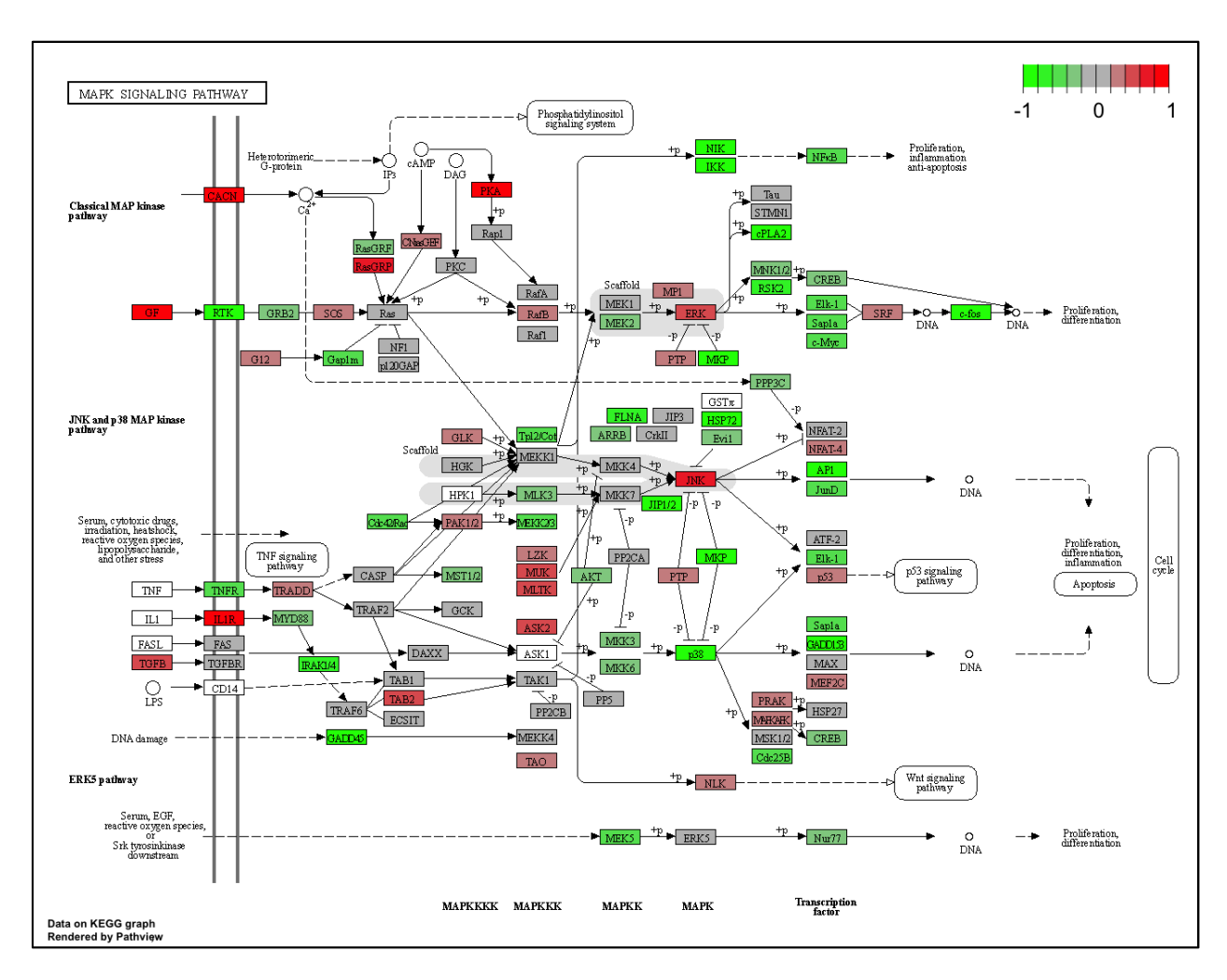


Figure S6. Upregulation of MAPK signaling KEGG pathway in SCVI-273 cardiac spheres cells after 3 days in the ISS μ G condition compared with the ISS 1G condition, related to Figure 6. KEGG, Kyoto Encyclopedia of Genes and Genomes. ISS 1G, the 1G condition on the International Space Station; ISS μ G, the microgravity condition on the International Space Station.

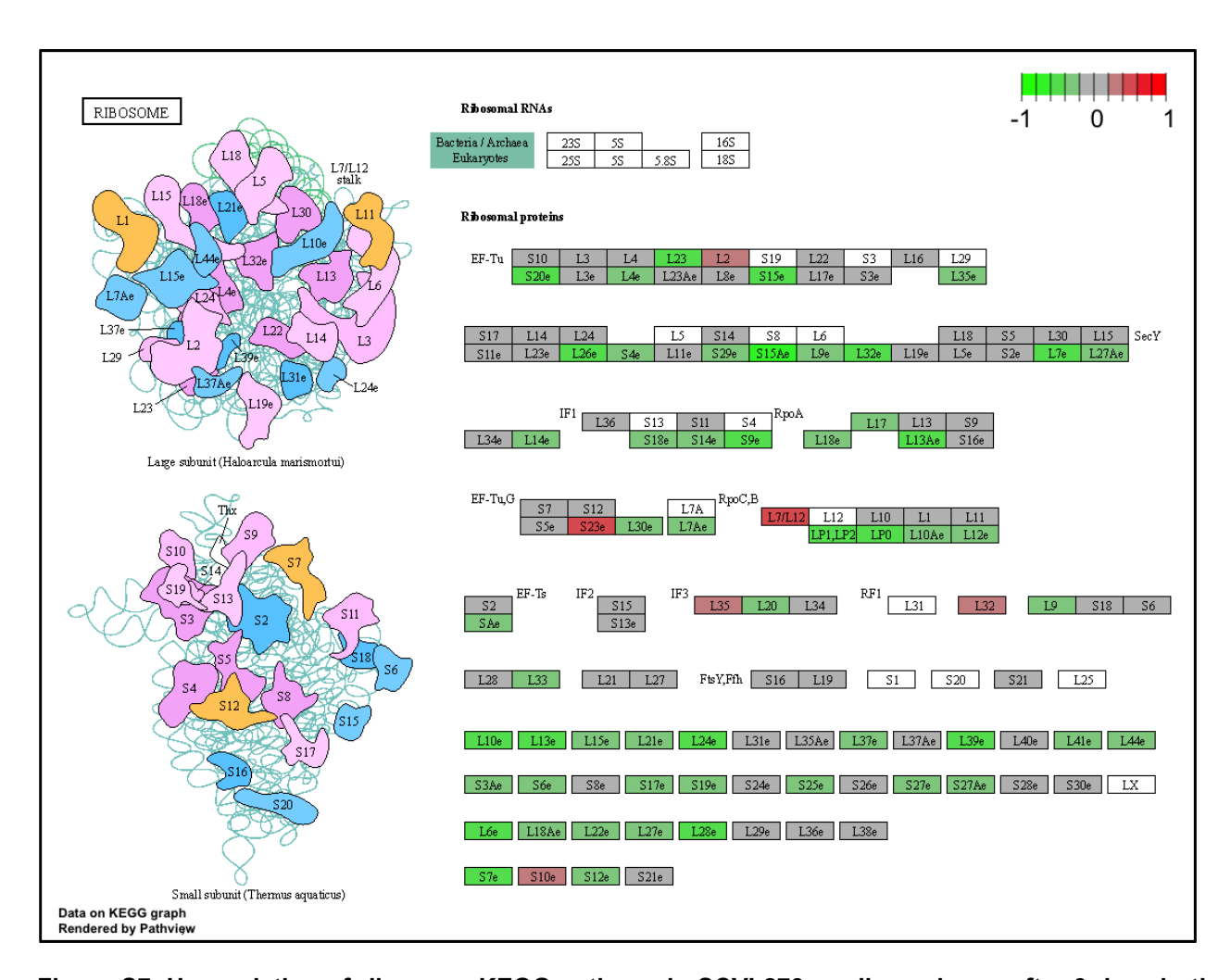


Figure S7. Upregulation of ribosome KEGG pathway in SCVI-273 cardiac spheres after 3 days in the ISS μ G condition compared to the ISS 1G condition, related to Figure 6. KEGG, Kyoto Encyclopedia of Genes and Genomes. ISS 1G, the 1G condition on the International Space Station; ISS μ G, the microgravity condition on the International Space Station.

Table S1. Top 60 genes significantly altered in SCVI-273 cardiac spheres after 3 days in the ISS μG condition compared with the ISS 1G condition.

Symbol	pared with the ISS 1 RefseqID	Gene Name	Log₂ (Fold change)	Adjusted P-value
Up-regulated			change,	
CCNB3	NM_033031	cyclin B3	7.24865	0.000447
PHETA2	NM_001002034	PH domain containing endocytic trafficking adaptor 2	6.28900	0.011831
MAML2	NM_032427	Mastermind like transcriptional coactivator 2	4.08855	0.021238
S1PR5	NM_001166215	Sphingosine-1-phosphate receptor 5	3.94179	0.041948
FOXI3	NM_001135649	Forkhead box I3	3.70948	0.040583
MDGA1	NM_153487	MAM domain containing glycosylphosphatidylinositol anchor 1	3.69290	0.041525
HTR7P1	NR_002774	5-hydroxytryptamine receptor 7 pseudogene 1	3.68840	0.015711
KRT18P39	NG_008329	Keratin 18 pseudogene 39	3.59350	0.025829
COL14A1	NM_001384947	Collagen type XIV alpha 1 chain	2.38044	0.004393
CDH4	NM_001252338	Cadherin 4	2.06183	0.024345
IL1R1	NM_000877	Interleukin 1 receptor type 1	1.95778	0.014894
ESPNL	NM_001308370	Espin like	1.91155	0.006634
RNF144A	NM_001349181	Ring finger protein 144A	1.81680	0.001494
GJA5	NM_005266	Gap junction protein alpha 5	1.74054	6.63E-05
NEK11	NM_001146003	NIMA related kinase 11	1.62646	0.041095
RAPH1	NM_001329728	Ras association (RalGDS/AF-6) and pleckstrin homology domains 1	1.59607	0.041924
CXCR4	NM_001008540	C-X-C motif chemokine receptor 4	1.54822	0.047314
PLEKHG5	NM_001042663	Pleckstrin homology and RhoGEF domain containing G5	1.47388	0.001073
ASXL3	NM_030632	ASXL transcriptional regulator 3	1.44174	0.008152
ENG	NM_000118	Endoglin	1.40961	0.000331
ARTN	NM_001136215	Artemin	1.31573	0.027638
RELN	NM_005045	Reelin	1.31012	0.017531
HSPG2	NM_001291860	Heparan sulfate proteoglycan 2	1.25137	0.021979
MPP7	NM_001318170	Membrane palmitoylated protein 7	1.23476	0.000836
TECRL	NM_001010874	Trans-2,3-enoyl-CoA reductase like	1.20932	8.98E-07
ACE2	NM_001371415	Angiotensin I converting enzyme 2	1.16266	6.01E-05
LINC01405	NR_036513	Long intergenic non-protein coding RNA 1405	1.15941	0.037903
ANKRD6	NM_001242809	Ankyrin repeat domain 6	1.12230	0.000288
KCTD12	NM_138444	Potassium channel tetramerization domain containing 12	1.12194	6.22E-08
MPPED2	NM_001145399	Metallophosphoesterase domain containing 2	1.09536	0.001695
Down-regulat		Jallan EQ obligation Page 1 Of	0.00440	0.000004
DTX3L	NM_138287	deltex E3 ubiquitin ligase 3L	8.02446	0.000264
SLC18A3	NM_003055	solute carrier family 18 member A3	7.23643	0.001875
SPTSSB	NM_001040100	serine palmitoyltransferase small subunit B	6.35097	0.001695
SERTM2	NM_001354473	serine rich and transmembrane domain containing 2	6.04704	0.003513

ABCB1	NM_000927	ATP binding cassette subfamily B member 1	5.88041	0.016678
NEURL1	NM_004210	neuralized E3 ubiquitin protein ligase 1	5.61512	0.001813
ADCYAP1R1	NM_001118	ADCYAP receptor type I	5.20116	0.020470
KCNK5	NM_003740	potassium two pore domain channel subfamily K member 5	4.84170	0.003182
ANGPT2	NM_001118887	angiopoietin 2	4.70263	0.012383
SLC13A2	NM_001145975	solute carrier family 13 member 2	4.48984	0.023994
NR3C2	NM_000901	nuclear receptor subfamily 3 group C member 2	4.30407	0.041447
CDH5	NM_001795	cadherin 5	4.02516	0.008447
LHX1	NM_005568	LIM homeobox 1	3.78842	0.001494
AL158212.3	AL158212	novel transcript, overlapping to VTI1A	3.78413	0.004772
FGD5	NM_001320276	FYVE, RhoGEF and PH domain containing 5	3.77704	0.000405
MBP	NM_001025081	myelin basic protein	3.17341	0.023584
GCNA	NM_052957	germ cell nuclear acidic peptidase	3.08693	0.022131
DUSP2	NM_004418	dual specificity phosphatase 2	2.98148	0.039780
IL6R	NM_000565	interleukin 6 receptor	2.95317	4.10E-06
DACT2	NM_001286350	dishevelled binding antagonist of beta catenin 2	2.89122	0.015902
MCHR1	NM_005297	melanin concentrating hormone receptor 1	2.87306	0.011433
HTRA3	NM_001297559	HtrA serine peptidase 3	2.58316	0.001695
H2BC4	NM_001381989	H2B clustered histone 4	2.47328	0.011865
AC109326.1	AC109326	TEC	2.46532	0.028379
SERPINE1	NM_000602	serpin family E member 1	2.31364	0.017119
HMOX1	NM_002133	heme oxygenase 1	2.31019	0.024004
PLEKHF1	NM_024310	pleckstrin homology and FYVE domain containing 1	2.20029	0.000496
BMP6	NM_001718	bone morphogenetic protein 6	2.19094	0.041095
EGR1	NM_001964	early growth response 1	2.18596	2.91E-05
CILP2	NM_153221	cartilage intermediate layer protein 2	2.15704	0.018451

ISS 1G, the 1G condition on the International Space Station; ISS μ G, the microgravity condition on the International Space Station.

Table S2. Composition of the CO₂-independent medium

Ingredients	Company Cat. No.	Volume (100 mL)
base CO ₂ -independent medium	Gibco 18045-088	Make up to 100 mL
B27 supplement with Insulin (50X)	Gibco 17504-044	2 mL
FBS	Hyclone SH30396-03	3 mL
HEPES (1M)	Gibco 15630-080	1.5 mL
GlutaMAX-I (100X)	Gibco 35050-061	1 mL
L-ascorbic acid 2-phosphate	Sigma A8960-5G	25 µl
sesquimagnesium salt hydrate	-	
(100 mg/mL, stock)		
non-essential amino acids (100X)	Gibco 11140-050	1 mL
antibiotic antimycotic solution (100X)	Sigma A5955-100ML	1 mL

Table S3. Primary antibody for immunocytochemistry

Target	Isotype	Supplier	Catalog	Dilution
α-actinin	Mouse IgG₁	Sigma	A7811	1:800
cTNI	Mouse IgG _{2b}	Millipore	MAB1691	1:200
cTNT	Mouse IgG₁	Fisher Scientific	MS295P1	1:200
NKX2.5	Rabbit IgG	Santa Cruz Biotech	SC14033	1:1600
Pan-cadherin	Mouse IgG₁	Sigma	C1821	1:500
Ki67	Mouse IgG₁	BD Bio	550609	1:50

Table S4. Secondary antibody for immunocytochemistry

Target	Fluorochrome	Supplier	Catalog	Dilution
Mouse IgG₁	Alexa Fluor® 488	Invitrogen	A21121	1:1000
Mouse IgG₁	Alexa Fluor® 594	Invitrogen	A21125	1:1000
Mouse IgG _{2b}	Alexa Fluor® 594	Invitrogen	A21145	1:1000
Rabbit IgG (H+L)	Alexa Fluor® 594	Invitrogen	A11012	1:1000

Table S5. Primers for qRT-PCR

Gene	Full name	Accession code	Primer
ACTN1	Actinin alpha 1	NM 001130004	Forward: AGGTGGGAGTTACACCATGC
	•	_	Reverse: ACATGCAGCCAGAAGAGGAC
ATP2A2	ATPase	NM 001681.4	Forward: TCAGCAGGAACTTTGTCACC
	sarcoplasmic/endoplasmic reticulum Ca ²⁺ transporting 2	_	Reverse: GGGCAAAGTGTATCGACAGG
ATP2B4	ATPase plasma membrane Ca ²⁺	NM_001001396	Forward: ATGACGAACCCATCAGACCG Reverse: TCAGTGCATCCCTTGAACGC
CASQ2	transporting 4 Calsequestrin 2	NM_001232	Forward: TTATGTTCAAGGACCTGGGC
07.10 42			Reverse: GCCTCTACTACCATGAGCCG
CCND1	Cyclin D1	NM_053056	Forward: GGCGGATTGGAAATGAACTT
	Gy 6 2 .	·000000	Reverse: TCCTCTCCAAAATGCCAGAG
CCND2	Cyclin D2	NM 001759	Forward: ACCTTCCGCAGTGCTCCTA
CONDL	3yo 22	14M_001700	Reverse: CCCAGCCAAGAAACGGTCC
GAPDH	Glyceraldehyde-3-	NM 001256799	Forward: CTGGGCTACACTGAGCACC
O/II DII	phosphate dehydrogenase	1411_001200700	Reverse: AAGTGGTCGTTGAGGGCAATG
IGF2	Insulin like growth factor 2	NM 000612	Forward: GTGGCATCGTTGAGGAGTG
	<u>9</u>		Reverse: CACGTCCCTCTCGGACTTG
MYH6	Myosin, heavy chain 6,	NM_002471	Forward: CTTCTCCACCTTAGCCCTGG
	cardiac muscle, alpha (α- MHC)	99	Reverse: GCTGGCCCTTCAACTACAGA
MYH7	Myosin, heavy chain 7,	NM_000257	Forward: CGCACCTTCTTCTCTTGCTC
	cardiac muscle, beta (β- MHC)		Reverse: GAGGACAAGGTCAACACCCT
MYL2	Myosin, light chain 2	NM_000432	Forward: CGTTCTTGTCAATGAAGCCA
		_	Reverse: CAACGTGTTCTCCATGTTCG
MYL7	Myosin, light chain 7	NM_021223	Forward: CTTGTAGTCGATGTTCCCCG
	, , ,	_	Reverse: TCAAGCAGCTTCTCCTGACC
RYR2	Ryanodine receptor 2,	NM_001035	Forward: CAAATCCTTCTGCTGCCAAG
	cardiac	_	Reverse: CGAAGACGAGATCCAGTTCC
TBX3	T-box transcription factor	NM 005996	Forward: CCCGGTTCCACATTGTAAGAG
	3	_	Reverse: GTATGCAGTCACAGCGATGAAT
TNNI1	Troponin I type 1	NM 003281	Forward: AGCATCAGGCTCTTCAGCA
	. ,,		Reverse: ACAGTCTGCAGTCTACGGCG
TNNI3	Troponin I3, cardiac type	NM_000363.5	Forward: CTCAAACTTTTTCTTGCGGC
	, 35, 3,60		Reverse: GTGAAGAAGGAGGACACCGA
TNNT2	Troponin T type 2, cardiac	NM_001001431	Forward: GCGGGTCTTGGAGACTTTCT
	,, , = _,		Reverse: TTCGACCTGCAGGAGAAGTT

Note: primers were retrieved from open access websites (http://primerdepot.nci.nih.gov/ or http://pga.mgh.harvard.edu/primerbank/)

SUPPLEMENTAL RESULTS

Preparation and characterization of cryopreserved cardiac progenitor spheres for the spaceflight experiment

For the spaceflight experiment, we prepared cryopreserved cardiac progenitor spheres from two hiPSC lines (Figure S1A-B). For the induction of cardiomyocyte differentiation, SCVI-273 hiPSCs were treated with small molecules (Lian et al., 2012) and IMR90 hiPSCs were treated with growth factors (Jha et al., 2015; Laflamme et al., 2007). On differentiation day 6, cardiac progenitor spheres were generated using microscale tissue engineering. After 24 h, cardiac progenitor spheres were cryopreserved in cryosyringes (Rampoldi et al., 2021). For quality assay of the cardiac progenitors, a frozen sample of the cardiac progenitor spheres was thawed and pre-tested for each cell line. Cardiac spheres were then transferred to suspension culture in a CO₂-independent medium with 10 μM ROCK inhibitor (Rampoldi et al., 2021); medium was partially changed (half volume) every other day, in order to mimic the conditions in the spaceflight experiment. Cardiac spheres started beating spontaneously by days 10-12 of differentiation in both cultures. A week after thawing, cardiomyocyte purity assay showed a very high percentage (>90%) of cells positive for NKX2.5 in cultures from both SCVI-273 and IMR90 hiPSC lines (Figure S1C-D). These results indicated that the cryopreservation and the CO₂-independent medium did not affect cell viability of the cardiac progenitor cells, and their ability to differentiate into cardiomyocytes. These pre-test results supported that the remaining samples were qualified to be sent to the ISS.

RNA-seq analysis reveals increased proliferation and differentiation during short-term exposure to space microgravity

A Gene Set Enrichment Analysis (GSEA) of GO terms showed that space microgravity upregulated genes associated with biological processes related to cardiac muscle cell development (GO:0055013, enrichment score 0.582, adjusted p-value 0.00025), muscle activity or cell contractions (actin-mediated cell contraction, GO:0070252 enrichment score 0.525, adjusted p-value 0.00027) (Figure 6B). Similar results were observed in GO terms of cellular components and molecular functions (Figure S2). The upregulated GO terms included structural constituent of muscle (GO:0008307, enrichment score 0.576, adjusted p-value 0.00324), or sarcomeric structure (A band, GO:0031672, enrichment score 0.728, adjusted p-value 0.00023) and voltagegated calcium channel activity involved in cardiac muscle cell action potential (GO:0086007, enrichment score 0.852, adjusted p-value 0.01514) or sodium channel activity (GO:0005272, enrichment score 0.574, adjusted p-value 0.01735). GO terms related to inflammation or apoptosis were downregulated, like regulation of tyrosine phosphorylation of STAT protein (GO:0042509, enrichment score -0.622, adjusted p-value 0.00123), MAP kinase phosphatase activity (GO:0033549, enrichment score -0.796, adjusted p-value 0.00113) and voltage-gated potassium channel activity (GO:0005249, enrichment score -0.575, adjusted p-value 0.00757). In addition, several downregulated GO terms were associated with processes, functions or components of non-cardiac cells, like nephron development (GO:0072006, enrichment score -0.528, adjusted p-value 0.00032), or neuronal cell body (GO:0043025, enrichment score -0.328, adjusted p-value 0.01439). These results were consistent with efficient differentiation and maturation of ISS µG cells into cardiomyocytes.

As shown in Figure 7A which is a detailed map showing upregulated GO terms of selected biological processes linked with specific differentially expressed genes, several upregulated genes in the ISS μG cells were involved in GO terms of cardiac muscle contraction (GO:0060048, enrichment score 0.460, adjusted p-value 0.00027) cardiac muscle tissue development (GO:0048738, enrichment score 0.415, adjusted p-value 0.00029) and muscle cell differentiation (GO:0042692, enrichment score 0.366, adjusted p-value 0.00034). The ISS μG cells had also upregulated GO term of cyclin-dependent protein serine/threonine kinase regulator activity (GO:0016538, enrichment score 0.461, adjusted p-value 0.02737) that was linked to upregulated genes of CCNB3 and CCND2. Among upregulated genes, CCNB3 had the highest increase in the ISS μG cultures (log2[fold change] = 7.25) (Table S1). CCNB3 is known to regulate the G2/M transition of mitotic cells (Li et al., 2019), whereas CCND2 regulates the G1/S and its overexpression was associated with increased survival and regeneration potency in hiPSC-CMs . In addition, cellular amino acid biosynthetic process (GO:0008652, enrichment score 0.525, adjusted p-value 0.00099) and the tricarboxylic acid cycle (GO:0006099, enrichment score 0.624, adjusted p-value 0.00115) were also upregulated, indicating that the ISS μG cells were metabolically more activate than the ISS 1G cells.

As shown in Figure 7B, several downregulated genes were correlated to GO terms related to tyrosine phosphorylation of STAT protein (GO:0007260, enrichment score -0.646, adjusted p-value 0.00070), response to interferon-gamma (GO:0034341, enrichment score -0.488, adjusted p-value 0.00032), and nuclear-transcribed mRNA catabolic process, nonsense-mediated decay (GO:0000184, enrichment score -0.508, adjusted p-value 0.00016). In addition, several genes connected to the GO term of positive regulation of vasculature development (GO:1904018, enrichment score -0.498, adjusted p-value 0.00031) were downregulated, including *ANGPT2* (Pöss et al., 2015) and *SERPINE1*. These genes were also associated with stress and cardiac diseases (Basisty et al., 2020; Simone et al., 2014).

The GO term of cellular response to calcium ion (GO:0071277, enrichment score -0.519, adjusted p-value 0.00454) was also downregulated in the ISS μ G cells (Figure 6B & Figure S2B). This GO term is related to cellular processes in which calcium is involved, including secretion, proliferation, enzyme production, and gene expression in addition to contraction. On the other hand, KEGG (Kyoto Encyclopedia of Genes and Genomes) pathway analysis of calcium signaling pathway (hsa04020, enrichment score 0.364, adjusted p-value 0.00900) indicated the upregulation of genes involved in contraction (including *CASQ* [calsequestrin 1], *RYR2, TNNC1* [troponin C1, slow skeletal and cardiac type] and *MLCK* [myosin light chain kinase], *CALM* [calmodulin] and *CAMK* [calcium/calmodulin dependent protein kinase]) (Figure S3A), which was consistent with the upregulation of several genes related to contractility. In addition, genes related to potassium channel activity, especially *KCNK5* (potassium two pore domain channel subfamily K member 5), were downregulated in the ISS μ G cells (Table S1).

KEGG enrichment analysis showed that several pathways were upregulated by space microgravity, including cardiac muscle contraction (hsa04260, enrichment score 0.406, adjusted p-value 0.02457) (Figure S3B), and adrenergic signaling in cardiomyocytes (hsa04261, enrichment score 0.485, adjusted p-value 0.00030), which is tightly connected to calcium signaling, cell contraction and cardiomyocyte maturation (Figure S4).

Among the most significantly upregulated genes (Figure 6A & Table S1), several were involved in cell cycle, like CCNB3. Therefore, we also investigated KEGG pathway associated with cell cycle (hsa04110) (Figure S5) that did not show up in the enrichment analysis. This pathway together with MAPK signaling pathway (hsa04010, enrichment score -0.362, adjusted p-value 0.01019) (Figure S6) showed downregulation of key checkpoint genes associated with DNA damage such as GADD45 (growth arrest and DNA damage). In addition, anti-inflammatory genes including $TGF\beta$ (transforming growth factor beta) and tumor suppressor gene p53 (tumor protein p53) were upregulated, while proto-oncogenes, including c-Myc (cellular $math{Myc}$), were downregulated in the ISS $math{\mu}G$ cells. In terms of cell cycle-related genes, mitosis block genes $math{CDC25C}$ (cell division cycle 25C) were downregulated, while $math{CDC14}$ (cell division cycle 14), which promotes mitotic exit, was upregulated in the ISS $math{\mu}G$ cells.

KEGG enrichment analysis also revealed that most of the genes associated with both small and large ribosomal subunit proteins were downregulated in the ISS μ G cells (Ribosome, hsa03010, enrichment score - 0.481, adjusted p-value 0.00059) (Figure S7).

SUPPLEMENTAL EXPERIMENTAL PROCEDURES

Cell culture and cardiomyocyte differentiation

Undifferentiated SCVI-273 hiPSCs (Stanford Cardiovascular Institute) and IMR90 hiPSCs (WiCell Research Institute) were cultured in a feeder-free hiPSC condition on Matrigel-coated plates, and fed daily with mTeSR™1-defined medium.

SCVI-273 hiPSCs were subjected to small molecule-induced cardiomyocyte differentiation (Lian et al., 2012), when compact colonies reached 90% confluence. Cells were initially treated on day 0 of differentiation with 6 μ M CHIR99021 in RPMI/B27 insulin-free medium. After 48 h, plain RPMI/B27 insulin-free medium was used for another 24 h. On day 3 of differentiation, cells were again treated with 5 μ M IWR1 in RPMI/B27 insulin-free medium for another 48 h.

IMR90 hiPSCs were subjected to growth factor-induced cardiomyocyte differentiation (Jha et al., 2015; Laflamme et al., 2007), when compact colonies reached >95% confluence. Cells were treated with 100 ng/mL activin A from differentiation day 0 till day 1 and 10 ng/mL bone morphogenic protein-4 (BMP4) from day 1 till day 4 in RPMI/B27 insulin-free medium (RPMI 1640 with 2% B27 minus insulin). Both cells lines were maintained before and during differentiation in a standard 37°C, 5% CO2 incubator.

Immunocytochemical analysis

Immunocytochemical analysis was conducted as described (Rampoldi *et al.*, 2021). Cardiac spheres were dissociated using 0.25% trypsin-EDTA and plated onto a Matrigel-coated 96-well culture plate at a density of 4×10⁴ cells/well and cultured for 2 days before fixation. On the day of the immunocytochemical staining, cells were washed with D-PBS, fixed in 4% (vol/vol) paraformaldehyde at room temperature for 15 min, and permeabilized in cold methanol for 2 min at room temperature. The cells were then blocked with 5% normal goat serum (NGS) in D-PBS at room temperature for 1 h and incubated with the primary antibodies in 3% NGS overnight at 4°C (Table S3). After the incubation with the primary antibodies, the cells were washed 3 times with D-PBS for 5 min each with gentle agitation to get rid of the unbound primary antibodies. The cells were then incubated with the corresponding conjugated secondary antibodies (Table S4) at room temperature for

1 h in the dark, followed by 3 times wash with D-PBS. The nuclei were counterstained with Hoechst 33342. Imaging was performed using an inverted microscope (Axio Vert.A1).

High-content imaging analysis

Cardiac spheres were dissociated using 0.25% trypsin-EDTA and plated onto a Matrigel-coated 96-well culture plate at a density of 4×10⁴ cells/well and cultured for 2 days to recover. After immunocytochemical staining, cells were imaged using an ArrayScan XTI Live High Content Platform (Life Technologies). Images were acquired and quantitatively analyzed using ArrayScan XTI Live High Content Platform (Life Technologies) (Rampoldi et al., 2019). Twenty fields/well were selected and 3 replicate wells per condition were imaged using a 10x objective. Acquisition software Cellomics Scan (Thermo Fisher Scientific) was used to capture images, and data analysis was performed using Cellomics View Software (Thermo Fisher Scientific). Images were analyzed with mask modifier for Hoechst-, NKX2.5-, and Ki-67-positive cells restricted to the nucleus.

Structural analysis of hiPSC-CMs

Under higher magnification with an inverted microscope (Axio Vert.A1), maturation of sarcomeric structures were examined in ISS μ G ad ISS 1G cell samples. Cardiac spheres were dissociated with 0.25% trypsin-EDTA, plated onto a Matrigel-coated 96-well culture plate at a density of 4×10⁴ cells/well and cultured for 2 days before fixation for immunocytochemistry. Cardiomyocytes were immunostained with α -actinin, a marker for myofibrillar Z-discs. The maturation of sarcomeric structures was evaluated by overall appearance of myofibrillar structure and categorize into 3 different levels as described previously (Nguyen et al., 2014; Ribeiro et al., 2015). Briefly, Score 1 are cells α -actinin positive but without clear sarcomeric striations; Score 2 are cells with a diffuse punctate staining pattern and some patterned striations in partial cell area; and Score 3 are cells with highly organized and well-defined myofibrillar structure with distinct paralleled bands of z-discs distributed throughout the cell area. The same cells were also analyzed by image processing software ImageJ, in order to measure difference between ISS μ G ad ISS 1G samples of cellular parameters like circularity (cell shape based on ratio between length and width), cell area and perimeter.

RNA-seg analyses

RNA was isolated using RNeasy Mini Kit (Qiagen) as per the manufacturer's instructions. RNA concentration was measured using a NanoDrop ND-1000 spectrophotometer (Thermo Fisher Scientific). RNA sequencing, quality control, and transcriptome mapping were done by Yerkes National Primate Research Center of Emory University. Total RNA quality was tested using an Agilent 4200 TapeStation and RNA 6000 Nano and Pico Chip (Agilent Technologies). RNA samples of triplicate ISS μ G and ISS 1G from Line 1 hiPSCs (SCVI-273) collected after a short-term exposure to microgravity were subjected for library preparation and sequencing.

Two nanograms of total RNA were used as input for cDNA synthesis, using the Clontech SMART-Seq v4 Ultra Low Input RNA kit (Takara Bio) according to the manufacturer's instructions. Amplified cDNA was fragmented and appended with dual-indexed bar codes using the NexteraXT DNA Library Preparation kit (Illumina). Libraries were validated by capillary electrophoresis on an Agilent 4200 TapeStation, pooled at equimolar concentrations, and sequenced on an Illumina NovaSeq 6000 at 100SR, yielding an average of 30 million reads per sample. Alignment was performed using STAR version 2.7.3a (Dobin et al., 2013) and transcripts were annotated using GRCh38. Transcript abundance estimates were calculated internal to the STAR aligner using the algorithm of htseq-count (Anders et al., 2015).

Differential gene expression analysis between two groups (ISS μ G vs ISS 1G) was performed in R programming environment (R package version 4.1.2) using DESeq2 (R package version 1.34.0) (Love et al., 2014). Gene annotation, Gene Set Enrichment Analysis, KEGG pathway analysis, and dot plot generation were performed using clusterProfiler (R package version 4.2.2) (Yu et al., 2012). Volcano plot was constructed using ggplot2 (R package version3.3.5) and genes were annotated on volcano plot using ggrepel (R package version 0.9.1). Chord plots were generated using enrichplot (R package version 1.14.1). KEGG diagrams were generated using pathview package (R package version 1.34.0). The resulting p-values were adjusted to control the False Discovery Rate (FDR). Genes with an adjusted p-value < 0.05 were assessed as differentially expressed.

Quantitative real-time RT-PCR (qRT-PCR)

For RNA samples after short-term exposure of space microgravity (3 days of cell culture on the ISS), intact cardiac spheres without cell dissociation were harvested and preserved in flight. For RNA samples after long-term exposure of space microgravity (3 weeks of cell culture on the ISS), intact cardiac spheres without cell dissociation were harvested and processed post-flight. RNA samples (5 ng each) were reverse transcribed using the iScript Reverse Transcription Supermix (Bio-Rad) as per the manufacturer's instructions to obtain cDNA, which was further processed in a Bio-Rad thermal cycler upon incubation with the reaction mixture at following temperature cycles: 25 °C for 5 min, 46 °C for 20 min, and 95 °C for 1 min. The reaction mixture was then diluted 15 times before further use for quantitative real-time PCR. Human-specific PCR primers (Table

S5) for genes examined retrieved from website the were an open access (http://pga.mgh.harvard.edu/primerbank/). Thermocycler reaction was set up using Applied Biosystems 7500 real-time PCR systems with the iTaq SyBr green master mix as follows: Initial denaturation step at 95 °C for 10 min; 50 cycles of 2 steps with 15 s of denaturation at 95 °C followed by 1 min of annealing at 60 °C; followed by a melting curve stage of 30 s at 95 °C and 15 s at 60 °C. All samples were normalized to the level of the housekeeping gene GAPDH (glyceraldehyde-3-phosphate dehydrogenase). Relative expression levels compared with control samples were presented as fold changes calculated by the $2-\Delta\Delta$ Ct method.

Calcium imaging

Cardiac spheres were dissociated using 0.25% trypsin-EDTA and plated onto a Matrigel-coated 96-well culture plate at a density of 2×10^4 cells/well and cultured for 2 days to recover. Live cell imaging of intracellular Ca^{2+} transient was performed using Fluo-4 AM, a cell permeant-fluorescent Ca^{2+} dye, as described. Cells were incubated with 10 μ M Fluo-4 AM for 20 min at 37°C followed by a 20 min wash at room temperature in Tyrode's solution (148 mM NaCl, 4 mM KCl, 0.5 mM MgCl₂·6H₂O, 0.3 mM NaPH₂O₄·H₂O, 5 mM HEPES, 10 mM D-Glucose, 1.8 mM $CaCl_2 \cdot H_2O$, pH adjusted to 7.4 with NaOH). Fluorescence was imaged over time using an ImageXpress Micro XLS System (Molecular Devices) at 20x objective and 30 frame per second. Fluorescence was measured from the entire cell region with excitation at 488 nm and emission at >500 nm. Analysis of Ca^{2+} recordings was performed with Clampfit 10.0 software (Molecular Devices).

SUPPLEMENTAL REFERENCES

Anders, S., Pyl, P., and Huber, W. (2015). HTSeq--a Python framework to work with high-throughput sequencing data. Bioinformatics (Oxford, England) *31*. 10.1093/bioinformatics/btu638.

Basisty, N., Kale, A., Jeon, O., Kuehnemann, C., Payne, T., Rao, C., Holtz, A., Shah, S., Sharma, V., Ferrucci, L., et al. (2020). A proteomic atlas of senescence-associated secretomes for aging biomarker development. PLoS Biol *18*. 10.1371/journal.pbio.3000599.

Dobin, A., Davis, C., Schlesinger, F., Drenkow, J., Zaleski, C., Jha, S., Batut, P., Chaisson, M., and Gingeras, T. (2013). STAR: ultrafast universal RNA-seq aligner. Bioinformatics (Oxford, England) 29. 10.1093/bioinformatics/bts635.

Jha, R., Wile, B., Wu, Q., Morris, A.H., Maher, K.O., Wagner, M.B., Bao, G., and Xu, C. (2015). Molecular beacon-based detection and isolation of working-type cardiomyocytes derived from human pluripotent stem cells. Biomaterials *50*, 176-185. 10.1016/j.biomaterials.2015.01.043.

Laflamme, M.A., Chen, K.Y., Naumova, A.V., Muskheli, V., Fugate, J.A., Dupras, S.K., Reinecke, H., Xu, C., Hassanipour, M., Police, S., et al. (2007). Cardiomyocytes derived from human embryonic stem cells in prosurvival factors enhance function of infarcted rat hearts. Nat Biotechnol *25*, 1015-1024.

Li, Y., Wang, L., Zhang, L., He, Z., Feng, G., Sun, H., Wang, J., Li, Z., Liu, C., Han, J., et al. (2019). Cyclin B3 is required for metaphase to anaphase transition in oocyte meiosis I. J Cell Biol *218*. 10.1083/jcb.201808088.

Lian, X., Hsiao, C., Wilson, G., Zhu, K., Hazeltine, L.B., Azarin, S.M., Raval, K.K., Zhang, J., Kamp, T.J., and Palecek, S.P. (2012). Robust cardiomyocyte differentiation from human pluripotent stem cells via temporal modulation of canonical Wnt signaling. Proc Natl Acad Sci U S A *109*, E1848-1857. 10.1073/pnas.1200250109.

Love, M., Huber, W., and Anders, S. (2014). Moderated estimation of fold change and dispersion for RNA-seq data with DESeq2. Genome Biol *15*. 10.1186/s13059-014-0550-8.

Nguyen, D., Hookway, T., Wu, Q., Jha, R., Preininger, M., Chen, X., Easley, C., Spearman, P., Deshpande, S., Maher, K., et al. (2014). Microscale generation of cardiospheres promotes robust enrichment of cardiomyocytes derived from human pluripotent stem cells. Stem Cell Rep 3. 10.1016/j.stemcr.2014.06.002.

Pöss, J., Ukena, C., Kindermann, I., Ehrlich, P., Fuernau, G., Ewen, S., Mahfoud, F., Kriechbaum, S., Böhm, M., and Link, A. (2015). Angiopoietin-2 and outcome in patients with acute decompensated heart failure. Clin Res Cardiol *104*. 10.1007/s00392-014-0787-y.

Rampoldi, A., Jha, R., Fite, J., Boland, G., and Xu, C. (2021). Cryopreservation and CO2-independent culture of 3D cardiac progenitors for spaceflight experiments. Biomaterials 269, 120673. 10.1016/j.biomaterials.2021.120673.

Rampoldi, A., Singh, M., Wu, Q., Duan, M., Jha, R., Maxwell, J.T., Bradner, J.M., Zhang, X., Saraf, A., Miller, G.W., et al. (2019). Cardiac Toxicity From Ethanol Exposure in Human-Induced Pluripotent Stem Cell-Derived Cardiomyocytes. Toxicol Sci *169*, 280-292. 10.1093/toxsci/kfz038.

Ribeiro, M., Tertoolen, L., Guadix, J., Bellin, M., Kosmidis, G., D'Aniello, C., Monshouwer-Kloots, J., Goumans, M., Wang, Y., Feinberg, A., et al. (2015). Functional maturation of human pluripotent stem cell derived cardiomyocytes in vitro--correlation between contraction force and electrophysiology. Biomaterials *51*. 10.1016/j.biomaterials.2015.01.067.

Simone, T., Higgins, C., Czekay, R., Law, B., Higgins, S., Archambeault, J., Kutz, S., and Higgins, P. (2014). SERPINE1: A Molecular Switch in the Proliferation-Migration Dichotomy in Wound-"Activated" Keratinocytes. Adv Wound Care 3. 10.1089/wound.2013.0512.

Yu, G., Wang, L., Han, Y., and He, Q. (2012). clusterProfiler: an R package for comparing biological themes among gene clusters. Omics *16*. 10.1089/omi.2011.0118.